Universidade de Lisboa

Faculdade de Ciências

Departamento de Biologia Animal

Novel nanomaterials against biofilm formation

Margarida João Ilhéu Viana de Queiroz

Dissertação

Mestrado em Biologia Humana e Ambiente

2013

Universidade de Lisboa

Faculdade de Ciências

Departamento de Biologia Animal

Novel nanomaterials against biofilm formation

Margarida João Ilhéu Viana de Queiroz

Dissertação

Mestrado em Biologia Humana e Ambiente

Orientadores:

Professora Doutora Margarida Moreira dos Santos

Professora Doutora Ana Maria Crespo

2013

Acknowledgments

Em primeiro lugar gostaria de agradecer a todos os que tornaram possível a elaboração desta dissertação. À minha orientadora, Doutora Margarida Moreira dos Santos pela sua boa orientação, disponibilidade, preocupação e partilha de conhecimentos essenciais a este trabalho. Ao Professor Doutor com Agregação Pedro Viana Baptista, pela disponibilização do laboratório e críticas construtivas que auxiliaram este trabalho. Gostaria de agradecer também à minha orientadora interna Professora Doutora Ana Maria Crespo.

Gostaria de agradecer a todos os colegas do CIGMH, laboratório 315, pelo acolhimento e contribuições ao longo desta investigação.

O maior agradecimento é à minha Mãe e ao meu Pai pelo apoio incondicional e conselhos fundamentais nesta etapa da minha vida, sem eles nada teria sido exequível. Aos Irmãos, Irmãs, Tios, Avós, Sobrinhos e TC pelo encorajamento e reconforto.

Agradeço ainda de forma muito especial a todos os meus amigos, cuja paciência, compreenção e palavras de motivação foram incansáveis.

Abstract

Microbial contamination is one of the major problems of modern society being an enormous public health threat. Nosocomial diseases are a manifestation of this threat, with high mortality and morbidity. Most of the nosocomial infections are due to biofilms, communities of microorganisms that are impermeable to antimicrobial agents. This resistance to antimicrobial agents presents a major concern, and thus the key solution to decrease nosocomial infections prevalence must be through prevention of biofilms formation. This is also the case for the food industry. The adopted strategy to solve this problem was through the utilisation of silver and silver:gold alloy-nanoparticles. These NPs were tested for their antimicrobial activity in biofilms formation, due to their unique characteristics inherent to their nanometer scale and to the composition of the silver component, already described as antibacterial. PHB/PHV films containing NPs were produced as novel biomedical material with antimicrobial properties.

Inhibition of *E. coli* and *S. aureus* biofilm formation was studied by the antimicrobial activity of Ag NPs and alloy-NPs, with different Ag:Au ratios, and also by their combined effect with antibiotics through a modified microtiter plate assay. We were able to conclude that 100% Ag NPs and 80% Ag:20% Au NPs inhibited *E. coli* biofilm formation and that all the produced NPs presented a synergic effect with antibiotics by inhibiting biofilm formation of both strains analysed. NPs biological activity while in a PHB/PHV matrix was evaluated by a contact test athwart halo observation. Silver NPs had antibacterial action for *E. coli* while in the polymer. NPs cytotoxicity was evaluated in HepG2 cells by a MTT assay and NPs ecotoxicity was evaluated through *D. salina* cell survivors after NPs exposure. The cytotoxic results showed that in general a Ag superior amount in the Ag:Au ratio caused a higher toxic effect. The ecotoxic results showed a high toxicity for silver NPs with 1 mg/mL Ag. The efficiency of these NPs may present a solution for the biofilms drug impermeability.

Keywords

Biofilm

Nanomaterials

Nanoparticles

Antimicrobial properties

E. coli

S. aureus

Resumo

Um dos maiores problemas da actualidade é a contaminação microbiana. Esta não só afecta a industria alimentar como também é a grande contribuinte para as infecções adquiridas em ambiente hospitalar. Como tal, é uma grande ameaça para a saúde pública. As doenças nosocomiais apresentam elevados valores de mortalidade e de morbilidade. A maior parte das infecções nosocomiais devem-se aos biofilmes. Os biofilmes são comunidades de microorganismos que são impermeáveis aos agentes antimicrobianos. Esta resistência aos agentes antimicrobianos é uma grande preocupação, consequentemente a prevenção da formação de biofilmes é a melhor solução. A estratégia utilizada para colmatar este problema foi efectuada através da utilização de nanopartículas de prata e de liga prata-ouro. Estas NPs podem ser inibidoras da formação de biofilmes por serem compostas por prata, conhecida como antimicrobiana, e por pertencerem à escala nano, logo têm propriedades únicas. O polímero PHB/PHV impregnado com NPs pode ter também propriedades antimicrobianas, e como tal, ser um novo nanomaterial biomédico para a solução deste problema.

A inibição da formação de biofilmes de *E. coli* e *S. aureus* em microplaca foi avaliada neste trabalho, com NPs Ag e NPs Ag:Au de diferentes composições em Ag:Au e também através do efeito sinérgico das NPs associadas a antibióticos. Concluiu-se que as NPs 100% Ag e as NPs 80% Ag:20% Au inibiram a formação de biofilmne de *E. coli*, e que todas as NPs utilisadas tiveram um efeito sinérgico com os antibióticios causando a inibição da formação de biofilmes para ambas as estirpes estudadas. A actividade antimicrobiana do compósito PHB/PHV-NPs foi avaliada através de um ensaio de contacto para a observação da formação de halos. As NPs 100% Ag tiveram efeito antimicrobiano em *E. coli*, quando impregnedas no polímero.

A citotoxicidade das NPs foi avaliada por um ensaio de MTT com células HepG2 e a ecotoxicidade das NPs foi avaliada através da contagem das *D. salina* sobreviventes à exposição às NPs. Em geral, quanto maior a % de prata

na composição das partículas maior é a citoxicidade associada. As NPs 100% Ag com 1mg/mL de Ag tiveram ecotoxicidade mais elevada. A eficiência destas NPs pode apresentar uma solução para a impermeabilidade dos biofilmes aos agentes antimicrobianos.

Palavras-chave

Biofilme

Nanomateriais

Nanopartículas

Propriedades antimicrobianas

E. coli

S. aureus

Table of contents

X

Table of figures

Table of tables

Abbreviations

Amp	Ampicillin
CFU	Colony forming units
CLSM	Confocal laser scanning microscopy
DMEM	Dulbecco's Modified Eagle Medium
DMSO	Dimethyl sulfoxide
FBS	Fetal bovine sérum
FCT/UNL	Faculdade de Ciencias e Tecnologia/Universidade Nova de Lisboa
FDA	Food and drug administration agency
HepG2	Human hepatocellular carcinoma (liver)
ICP	Inductively coupled plasma
IST/UTL	Instituto Superior Técnico/Universidade Técnica de Lisboa
Km	Kanamycin
LB	Luria–Bertani
MH	Mueller–Hinton
MIC	Minimum inhibitory concentration
MTT	3-(4,5-dimethylthiazol-2-yl)-2,5-diphenyltetrazolium bromide (tetrazolium dye)
NPs	Nanoparticles
OD	Optical density
PBS	Phosphate buffered saline
PHA	Polyhydroxyalkanoate

PHB/PHV	Polyhydroxybutyrate/polyhydroxyvalerate
PVC	Polyvinyl chloride
SEM	Scanning electron microscopy
TEM	Transmission electron microscopy
TSB	Tryptic Soy Broth

Chapter 1 – Introduction

Nowadays, microbial contamination is an important issue that affects the public heath through the hospital-acquired diseases and the food industry. Inherent to this problem are also economic consequences to the affected subjects [1,2,3].

One of the most preoccupying consequences of this issue are the nosocomial diseases, also known as hospital-acquired infections. These kinds of infections are a growing concern to the modern society because they affect people all over the world and have a high mortality rate. Nosocomial infections are usually due to biofilms, and consequently more difficult to treat, with several biological mechanisms that are not completely understood. In addition, these microbial communities can be formed by almost every species of bacteria [2,4,5].

Nanotechnology is a subject in great study expansion because of the several applications that it can be associated with. Nanomaterials such as noble metal-nanoparticles may present many advantages compared to the bulk material, because of their unique physico-chemical properties. Silver NPs and Ag:Au NPs present antimicrobial properties that could represent a good alternative to the ineffective antibiotics. A disadvantage of these NPs may be the toxicity inherent to them due to its compositions in silver, and the high concentrations required [6,7,8].

Polymeric materials are widely used in the biomedical field. As such, the possibility of conferring additional antimicrobial properties to these materials should present advantages, since they are already used in biomedical instruments. polyhydroxybutyrate/polyhydroxyvalerate is a polymer with common using good characteristics as malleability and though. A creation of a composite PHB/PHV polymer with NPs should present benefits to the bulk materials [9,10].

1.1 The problem *versus* the solution

It is known that the nosocomial diseases are a public health threat mainly caused by biofilms, and so, very difficult to manage because biofilms are

impermeable to antimicrobial agents. The best option to reduce this problem must be through prevention.

Antimicrobial effects with Ag NPs and Ag:Au alloy-NPs were studied in this work with the purpose of inhibiting *Escherichia coli* and *Staphylococcus aureus* biofilm formation. A synergic effect of these NPs with kanamycin and ampicillin was also studied because an enhancement of the antibacterial activity could occur and consequently, biofilm growth inhibition would be observed [11]. The NPs cytotoxicity and ecotoxicity should be evaluated, having in mind the future utilisation of this nanomaterials in the biomedical field or the food industry [6,12]. A PHB/PHV film is a suitable matrix to contain NPs, because it has desirable characteristics for biomedical applications and is FDA (US Food and Drug Administration) approved. As a result, composite materials containing the polymer and NPs should be evaluated [9,10].

The possibility of creating nanomaterials with antimicrobial properties that could inhibit biofilm formation must have an important role in nosocomial infections prevention and control of food-borne diseases.

1.2 Objectives

- Synthesis and characterisation of different types of Ag NPs or Ag:Au alloy-NPs
- Development of systems for biofilm formation
- Characterisation of the obtained biofilms
- Evaluation of antimicrobial properties of the NPs produced on biofilm formation
- Evaluation of a possible synergic effect of the NPs with antibiotics
- Evaluation of the antimicrobial properties of the polymers synthesised when combined with the NPs produced
- Evaluation of the cytotoxic effects of NPs
- Evaluation of the ecotoxic effects of NPs

1.3 Methodology

The first step was to study the inhibition of biofilm formation by performing a literature research. Then, specific objectives were established (see previous section) and an appropriate strategy was also established in order to achieve them. This resulted in a set of interlinked processes described in Fig. 1.

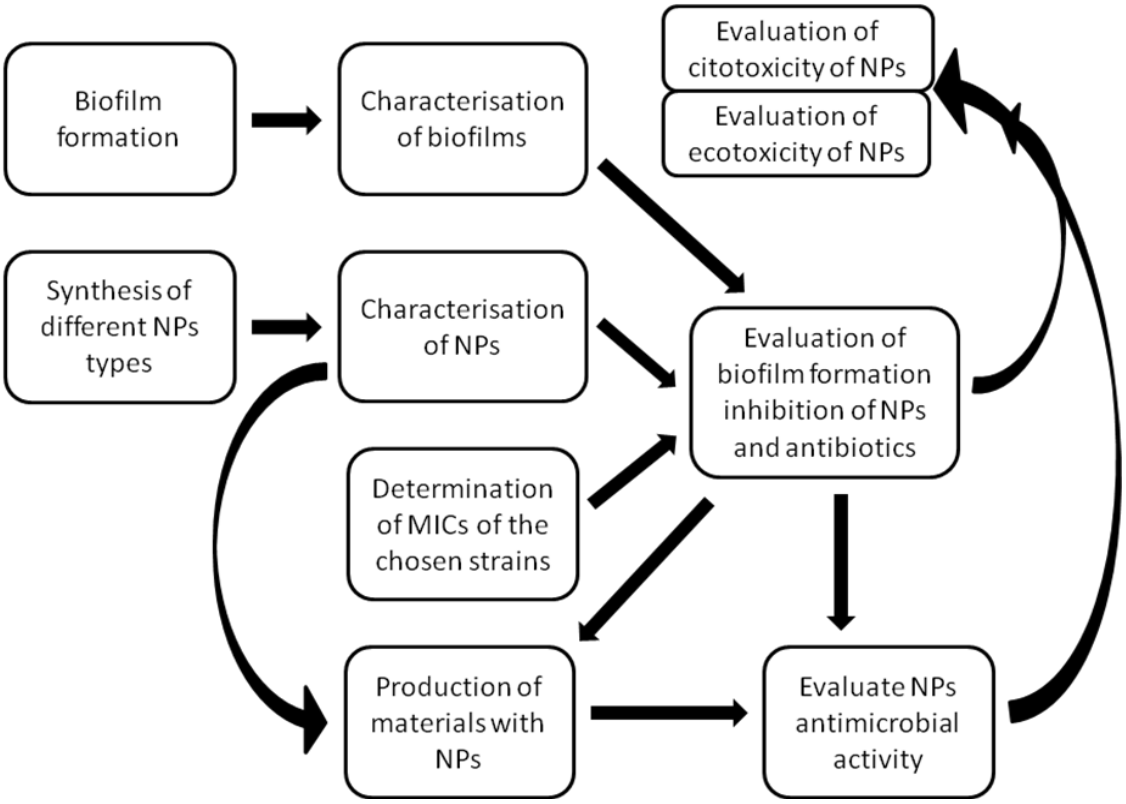

Fig. 1 Methodology of the this work by an end-to-end process

The final goal of producing novel nanomaterials against biofilm formation was only possible due to these sequential and complementary processes.

Chapter 2 – State of the Art

2.1 The problem of microbial contaminations

One of the serious problems of modern society is microbial contamination. This is an issue that affects not only the public heath but also the economy. Nosocomial infections are a reflection of the nuisance caused by this problem in health institutions. Microbial contamination affects the food industry too in primary and final products. Prevention must be the key to these problems resolution [1,2].

Nosocomial disease is the designation of the infection acquired by a person while in a hospital. These hospital-acquired infections affect over 1.4 million people in the world. This public health threat is of high magnitude because it can occur worldwide, regardless of the country's development, and the values of morbidity and mortality associated to them are high [2]. There are several factors that contribute to the development of the nosocomial diseases: 1) the biology of the infectious agents (bacteria, virus, fungus and parasites), that leads to a quick increase of their frequency; 2) the multi-resistance to antibiotics acquired by these organisms due to their fast development and expropriated prophylaxis on patients; 3) the heath institution users that may have advanced age or a compromised immune system, due to an underlying disease; 4) the invasive techniques that the patients might be subject to; 5) the hospital environment that has a lot of different infectious microorganisms, which makes it possible to have cross contamination between people, surfaces and equipments [2]. There are several nosocomial diseases. However, the most common are the infections associated with surgical wounds (dental or orthopaedic implants), with the urinary tract and with the respiratory tract [2,4]. The public health threat posed by the nosocomial diseases has an economic burden associated, because when a patient acquires a nosocomial infection his length of stay in a health care facility increases, as well as the use of drugs and laboratory/diagnostic work [2,3].

2.2 Biofilms

Biofilms can be defined as a form of growth where a community of microorganisms attach to a biotic or abiotic surface. These agglomeration of microorganisms are embedded in a matrix that is composed of extracellular DNA and extracellular polymeric substances, as polysaccharides and proteins [5,13,14,15,16]. Bacteria's characteristics such as hydrophobicity and charge may be an influence to the surface chosen for cells adhesion. A mature biofilm structure is very complex and has characteristics as antibiotic and UV-light resistance, high genetic exchange rates, biodegradability, nutrient sequestration and high production of secondary metabolites [5,14].

99% of the microorganisms on Earth can compose biofilms forms that can be multi-species or one single species, and 99% of microbial life is in a biofilm form. Hence there are lots of complicated symbiotic interactions between the organisms in a biofilm form, which may be regulated by a quorum sensing mechanism. [5,15,16].

The processes involved in a biofilm lifecycle are not totally understood yet, however, four stages have been reported: initiation, maturation, maintenance and dissolution [5,13]. The first stage of biofilm formation is the initiation, which may be essentially driven by environmental factors as nutrient availability/unavailability, osmolarity and pH. Biofilm development behaviour is controlled by genetic pathways and chemical cell-surface interactions. It is already been studied that microorganisms have an increased expression of exopolysaccharides when they turn to a biofilm form of growth, but none of the other physiological and functional alterations that they suffer to become a community adherent in a surface has been fully understood [5]. Biofilm disassembly includes many steps, such as extracellular matrix degradation and physiological changes. This may be driven by starvation/nutrient depletion, overexpression of some enzymes, accumulation of wastes, underexpression of exopolysaccharides or by antimicrobial agents. However, these processes are not completely understood yet [5,13].

Nosocomial infections are, in general, caused by a one single species biofilm. Biofilm dispersion may enhance the threat of a nosocomial disease because the release of the infectious agents might cause embolic episodes or sepsis [5,16].

Several methods may be used to investigate biofilms, including microscopy methods (SEM, TEM, CLSM,…) and colorimetric methods (vitality dyes – fluorescence; biomass determination dyes – crystal violet and safranin) [4,17,18].

2.3 *Escherichia coli* and *Staphylococcus aureus* strains

In this dissertation we will study biofilms of two laboratory model bacteria, the Gram-negative *Escherichia coli* and the Gram-positive *Staphylococcus aureus* [2].

Gram-negative bacteria like *E. coli* have a peptidoglycan layer between two membranes, which gives it firmness. The outer membrane is porous and composed by phospholipids, proteins and polysaccharides that increase its permeability (Fig. 2) [19].

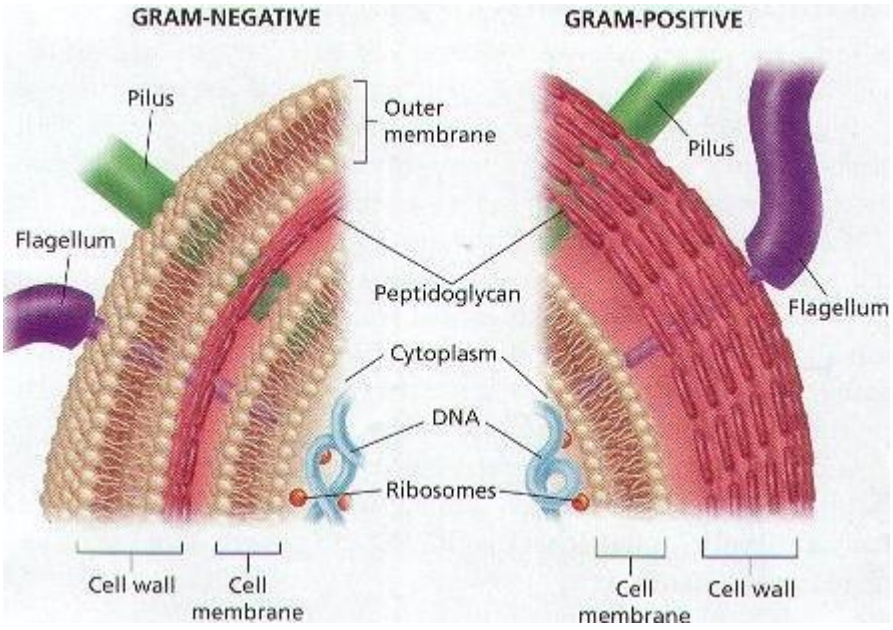

Fig. 2 Differences between Gram-negative and Gram-positive bacteria [19]

E. coli can be found in various environments and usually in human intestines. These bacteria play an important role in the health of the intestinal tract.

Nevertheless, *E. coli* it may present pathogenic strains and cause diseases, such as diarrhea, respiratory illness or pneumonia [20].

S. aureus is regularly found in human skin and nose and may also present pathogenic strains. This bacterium is the main cause of several nosocomial diseases like pneumonia, bacteremia, endocarditis, septic arthritis, skin infections, meningitis, osteomyelitis and surgical site infections. *S. aureus* is responsible for 46% of nosocomial infections and its biofilm for 54% of them. This problem is enhanced due to the fact that *S. aureus* is resistant to several antibiotics (for example: penicillin and ampicillin) [3,13,21].

In conclusion, these two bacteria are a big problem to public heath because they may present pathogenic strains, multi-resistant strains and may be frequently a cause of nosocomial infections acquired by ventilation or contact with contaminated materials [3,4,11].

2.4 Nanotechnology

The creation of useful devices, materials and systems at nanometer scale is named as nanotechnology. To be considered a nanomaterial, it has to be between 1-100 nm in at least one dimension [7]. Nowadays, nanotechnology is having an exponential development because it allows several advantages in the industrial sector. Applications of nanoparticles are widely studied in the biomedical field because of their unique physico-chemical properties due to the size related properties like different surface/volume ratio, the possibility of having different shapes, their compositions and the possibility to functionalise with organic or inorganic molecules [6,7,8,22].

Nobel metal-NPs have a specific optical characteristic, light absorbance in the UV-Vis. range due to the surface plasmon resonance [7,8,22]. A surface plasmon resonance band is represented by an intense absorption of light driven by the excitation of electrons after an electromagnetic wave that propagates along the surface of the conductive metal. In other words a surface plasmon resonance band is created by the collective oscillation of the conduction electrons on the NPs surface after excitation by light [7,8,22]. These resonance bands can be

modulated by the NPs metal composition, size and shape (Fig. 3). NPs with different compositions can modulate their surface plasmon resonance band by their conformation. Alloy-NPs only present one characteristic peak of absorption while core-shell-NPs presents two distinct bands characteristic of each pure metal [7,8,22]. The surface plasmon resonance band depends on inter-particle distance. Consequently, when the NPs aggregate (electrostatic repulsive forces are replaced by Van-der-Waals attractive forces), they suffer a colour change and the plasmon band red-shifts [7,8,11,23].

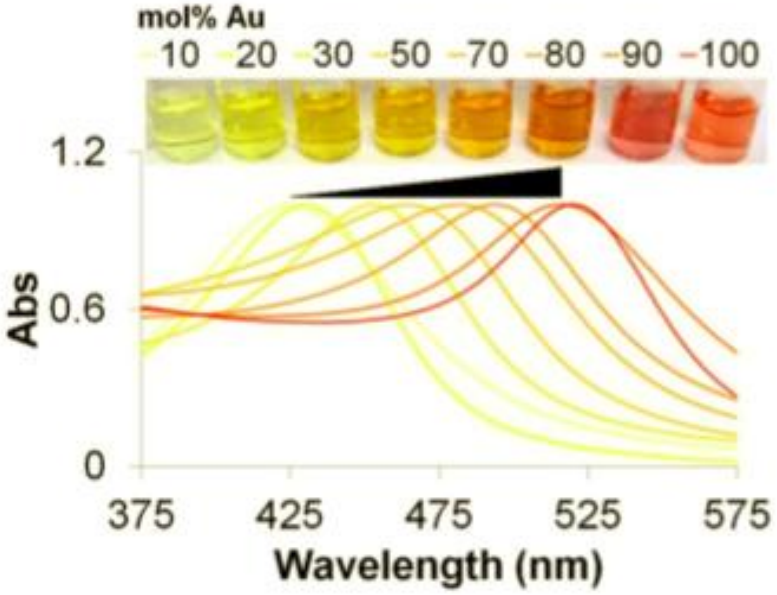

Fig. 3 Example of localized surface plasmon resonance modulation through different NP compositions. The localized surface plasmon resonance absorption band of gold/silver alloy NPs increases to longer wavelengths with increasing amounts of gold [7]

There are quite a few methods of nanoparticle synthesis to obtain different sizes, shapes and compositions [7]. One of the methods to obtain Ag:Au-alloy NPs is through the co-reduction of $AgNO_3$ and $HAuCl_4$ with sodium citrate as a reducing and capping agent [6,7,8,11,22]. The citrate stabilises the colloidal suspension, but this stabilisation is not strong [6,7].

To characterise NPs by their shape and size distribution microscopic methods for imaging (SEM or TEM) may be used. NPs spectra in UV-Vis. range

characterise their surface plasmon resonance band. The elemental composition of NPs may be determined by ICP [4,11,17].

There are several factors that influence NPs antimicrobial activity, including their chemical composition, size, shape and superficial charge. Gold NPs are widely used for molecular diagnosis, imaging drug delivery and therapeutics [7,22], while silver NPs are commonly used for their antimicrobial properties [6,8,11,14,17,18]. NPs mechanisms of action are not very clear, yet their physical structure is proposed as an important factor, because of the possibility of destruction/penetration of the cellular membrane. Another proposed mechanism of action is through the release of metal ions that interfere with microorganisms function [6,11,17,18].

Since ancient times, biocide properties of silver are known. Nowadays these properties are also associated with silver NPs. As such, Ag NPs became a useful resource to medicine, although silver may be toxic in certain amounts, which might be a handicap. The antimicrobial activity of silver NPs has been already studied for some Gram-negative and Gram-positive bacteria resistant to antibiotics, fungus and virus and in planktonic or biofilm form [4,6,11,14,17,18]. Yet the mechanism of this antimicrobial action is difficult to explain. One mechanism proposed for the antimicrobial action of the NPs is through the slow dissolution of silver ions [6,14]. Some authors suggest a maximum antimicrobial activity for Ag NPs with 50 nm triangular shapes by Ag^+ interference with the cell membrane integrity, with the respiratory chain and with DNA replication [17].

Ag:Au-alloy NPs have a biological action which comprises properties of both metals [6,11,22]. Gold is described as an inert compound easily functionalised with organic molecules. Silver, however, is toxic but presents good antimicrobial and anti-adhesive properties for some species such as *E. coli* and *S. aureus* [4,6,17]. The Ag:Au-alloy NPs might present antibacterial properties and a lower toxicity when compared with silver NPs, insofar as the amount of the toxic metal silver is lower [6,11,22].

Nanoparticles potential toxicity is an actual concern due to their high utilization in nanotechnology. Ag NPs toxicity has already been studied, but little is known

about Ag:Au-alloy NPs [24]. It is suggested that several factors affect Ag NPs cytotoxicity, such as their preparation method, size, shape and capping agent [12,14,24,25]. Cell uptake may be also be influenced by the NPs concentration, incubation time and aggregation [6,23,25]. This toxicity may be due to the cell wall permeability disturbance, cell penetration, generation of toxic radicals as reactive oxygen species and Ag^+ slow dissolution. Silver ions slow dissolution may interact with cell biomolecules, nucleic acids, metabolic enzymes and wall components [6,14]. An ecotoxic evaluation may also be important, because not only the metals that compose the NPs may be toxic, as silver, but also because the capping agents may lead to environmental concerns [12,14].

As previously mentioned, microorganisms may develop antibiotic resistance, thus NPs with antimicrobial properties present a good alternative to antibiotics [11,17,18]. Kanamycin is an antibiotic of the first line of treatment that was used to treat *E. coli* infections. However due to the difficult administration and toxic effects in normal concentrations this drug is not longer used. Ampicillin was also generally used in clinical practice as an antibiotic of the first line of treatment for *S. aureus* infections, but many bacterium strains are now resistant to this drug. The possibility of enhancing the antimicrobial action of a fallen antibiotic with NPs by a synergic action may be a good strategy to the reutilisation of them.

2.5 Polymers with nanoparticles

The antimicrobial properties of Ag NPs and Ag:Au-alloy NPs may be different according to their physical form. Not only NPs may have antimicrobial activity in suspension, but also when they are part of a polymeric material.

Polyhydroxyalkanoates are polyesters that can be synthesised by many bacteria, through intracellular accumulation of carbon and processed by extrusion, injection or compression moulding. The PA used in this study was polyhydroxybutyrate/polyhydroxyvalerate. This is a thermoplastic co-polymer composed by PHB and PHV; as such it includes features of both PHB and PHV. PHB has the characteristic of being able to be degraded and reabsorbed in the human body, and the biocompatibility that makes it suitable as a matrix for bioactive components. However, this polymer tends to be brittle. PHV is softer

and tougher than PHB. The major advantage of combination of these polymers is the flexibility and toughness inherent of the co-polymer. PHB/PHV is a material with high potential for biomedical applications due to its biodegradability [9,10]. The characteristics of the co-polymer described a suitable to contain NPs with the purpose of creating a composite material with antimicrobial properties.

Chapter 3 – Experimental Methods

3.1 Synthesis and characterisation of NPs

Ag NPs and Ag:Au-alloy NPs were synthesised by citrate co-reduction of $AgNO_3$ (MERK, Germany) and $HAuCl_4.3H_2O$ (Sigma-Aldrich, USA), a method that was adapted from the original of Turkevich [22,26]. In brief, 250 mL of a $AgNO_3$ solution or $AgNO_3$ and $HAuCl_4.3H_2O$ solution prepared in milli-Q H_2O (Millipore MilliQ system (Merck KGaA, Germany)) were heated in a 500 mL round-bottom flask with stirring. Once the solution refluxed, 25 mL of sodium citrate tribasic dihydrate (Sigma-Aldrich) were quickly added. After 15 min, the heating was turned off and the solution was left at room temperature overnight with continuous stirring. The solution of NPs was stored at room temperature in the dark.

Five different types of NPs with different metal compositions, Ag:Au ratio, and different citrate concentrations were produced. Table 1 summarises the concentration of reagents used in the NPs synthesis.

Table 1 Reagents used in NPs synthesis

NPs type	$AgNO_3$ (mg/L)	$HAuCl_4.3H_2O$ (mg/L)	Sodium citrate (mM)
1	78.5	0.0	38.8
2	58.9	45.5	38.8
3	39.3	90.9	38.8
4	19.6	45.5	34
5	19.6	45.5	34

For each type of NPs the synthesis was repeated three times, and pooled together, to reach the necessary volume for all the experiments described in this thesis. NPs types 4 and 5 were synthesised with the same concentration of silver and gold, because in the course of the experiments a larger volume was necessary.

NPs were characterised by UV-Vis. spectrophotometry in a Uvmini-1240 Shimadzu and in a micro plate reader Infinite M200 Tecan. Their elemental

composition was determined by ICP outsourced at REQUIMTE at FCT/UNL. TEM imaging was used to determine the average size of the particles, outsourced at iST at IST/UTL.

3.2 Strains and maintenance

Two different model bacteria were used, the Gram-negative *Escherichia coli* DH5α and the Gram-positive *Staphylococcus aureus* NCTC8325-4. *E. coli* was grown at 37ºC in LB medium (10 g/L bacto-tryptone (Bacto™), 5 g/L yeast extract (Bacto™), 1 g/L NaCl (Sigma-Aldrich), pH 7.5). *S. aureus* was grown at 37ºC in TSB medium (Bacto™) (17 g/L bacto-tryptone, 3 g/L bacto soytone, 2.5 g/L dextrose, 5 g/L NaCl, 2.5 g/L K_2HPO_3, pH 7.3). Stocks cultures were kept at -80ºC with 15 % glycerol (PRONALAB). The working stocks were kept at 4ºC on Petri dishes containing growth media solidified with agar (15 g/L agar-agar (Sigma-Aldrich)) and replaced every 3 weeks.

The pre-inoculum was prepared by dispersion of one single colony in 5 mL of media and overnight incubation at 37ºC.

3.3 Biofilm formation

3.3.1 On microscope slides (glass)

20 mL of medium supplemented with 0.05% D-(+)-glucose (Sigma-Aldrich) was inoculated with 1 µL of fresh culture of *E. coli* or *S. aureus* and placed in a Petri dish with a sterile microscope slide on the bottom. The Petri dishes were incubated at 37ºC. The slides were removed at different time points, washed with distilled water and dried with paper towels. Then, two 10 µL drops of crystal violet 2% (Sigma-Aldrich) were placed in a large lamella upside down which was covered by the slide. The biofilm formed was characterised by optical microscopy in microscope Leica DMR with a Leica DFC320 camera. This experiment was performed in duplicate for each time point for every independent experiment. At least two independent experiments were performed.

3.3.2 On microtiter plates (PVC)

After a protocol optimization, biofilm formation was obtained in a 96-well microtiter plate with an inoculum of 1:10000 (*E. coli* or *S. aureus*) with 1% glucose, for a total volume of 200 µL, which was kept with agitation at 37ºC for 24 h or 72 h. Negative control were not inoculated. Each condition was tested in triplicate for every independent experiment. At least two independent experiments were performed.

The evaluation of biofilm formation was done by a colorimetric test with crystal violet. In brief, the content of the wells was stirred, removed and washed three times with 250 µL of sterile physiological saline solution 0.9% to withdraw the non-adherent bacteria. The following step was the fixation of the adherent microorganisms with methanol 99% (VWR® PROLABO®) for 15 min followed by the supernatant removal. 200 µL of crystal violet 2% was added and after 5 min the plate was washed with running water. Then, the plate was dried with compressed air and 160 µL of glacial acetic acid 33% (MERK) was added for the homogenisation of stained microorganisms. The absorbance was measured at 570 nm in a micro plate reader Infinite M200 Tecan.

3.4 Determination of MICs

MICs were determined in a 96-well microtiter plate with kanamycin (NZYTech) for *E. coli* DH5α and with ampicillin (Sigma-Aldrich) for *S. aureus* NCTC8325-4. The protocol used was an adaption from CLSI Antimicrobial Susceptibility Testing Standards (CLSI, USA), using sequential two-fold dilutions over the wells for a fresh inoculum of 1:10000.

MICs were the lower antibiotic concentration that inhibited growth. They were determined in duplicate by visual observation after 24 h and 48 h of incubation at 37ºC.

3.5 Biofilm growth inhibition in a 96-well microtiter plate

3.5.1 Inhibition of biofilm growth by antibiotic activity

The biofilm formation protocol described in section 3.3.2 was used with a modification: antibiotic was added before incubation with a concentration of the MIC, 50% MIC and 25%. Every assay was performed at least in duplicate.

3.5.2 Inhibition of biofilm growth by NPs activity

The biofilm formation protocol described in section 3.3.2 was used with a modification: NPs were added before incubation. 6.75 mL of NPs per well were concentrated to 10 µL through two centrifugations at 14500 rpm for 20 min in a micro centrifuge Certomat IS Sartorius. Every assay was performed at least in duplicate.

3.5.3 Inhibition of biofilm growth using antibiotics and NPs together

This assay was the combination of the two described before in sections 3.5.1 and 3.5.2. The biofilm formation protocol described in section 3.3.2 was used with two modifications: antibiotic with a concentration of the 50% MIC and 25% MIC was added before incubation simultaneously with 10 µL of NPs per well that were concentrated from 6.75 mL.

3.6 PHB/PHV films

3.6.1 Preparation of PHB/PHV films

0.5 g PHB/PHV were dissolved in 75 mL chloroform (Sigma-Aldrich, contains ~ 1% ethanol as stabilizer) containing 0.5% Tween 20 (Sigma-Aldrich) with continuous stirring at 50ºC overnight. Then, about 19.5 mL of the homogenous mixture was placed on a glass Petri dish not completely covered and the solvent was evaporated overnight. The films that were made had approximately 0.13 g of polymer.

3.6.2 Preparation of PHB/PHV films with NPs

To produce PHB/PHV films containing NPs, 10 µL of NPs concentrated from 6.75 mL by two centrifugations at 14500 rpm for 20 min in a micro centrifuge Certomat IS Sartorius were used in the solution before it was being placed into the Petri dish.

3.6.3 Antimicrobial activity of PHB/PHV films

An overnight grown culture was spread using a cotton swab on a Petri dish with MH medium (DIFCO) (2 g/L beef extract powder, 17.5 g/L acid digest of casein, 1.5 g/L soluble starch). A square of PHB/PHV film with about 30 mg (approximately 1 cm long) was placed on top of the culture. The plates were incubated at 25ºC and 37ºC. After 24 h they were visually inspected. Duplicate determinations were made.

3.7 Cytotoxicity of NPs

To evaluate the cytotoxicity of the produced NPs, the MTT assay was performed in triplicate. HepG2 cells were maintained in a T75 flask with DMEM medium (Life Technologies, DMEM (1x) GlutaMax supplemented with 10% FBS and 1% Penicillin/Streptomycin) renewed every week at 37ºC. All assays were performed between cells passage number 10 and 15. The first step was to wash HepG2 cells with 5 mL of PBS (8 g/L NaCl (MERK), 0.2 g/L KCl (MERK), 1.44 g/L $NaH_2PO_4.H_2O$ (MERK), 0.24 g/L $KHPO_4$ (MERK), pH 7.4) and then 2 mL of trypsin/EDTA (1x) (Life Technologies) were added for 5 min to release the cells from the bottom of the flask. Then 6 mL of DMEM medium were also added to neutralise the trypsin/EDTA. The 8 mL suspension was well mixed and placed in a falcon tube. To determine the cell number in 1 mL, 10 µL of this mixture was placed in an eppendorf with 10 µL of trypan blue 0.5% (w/v) (Seromed®). 10 µL of this suspension was put in a counting chamber (NEUBAUER improved, 1 mm; 0.0025 mm^2) that was observed with an optical microscope (Nikon TMS Japan, 0.2 A). The dilution of cells was performed with DMEM in a new falcon tube. 100 µL of cells were incubated at 37ºC for 24 h in a 96-well microtiter plate. The DMEM was removed and replaced with fresh

media previously incubated at 37ºC. NPs of different compositions and concentrations were added. After two centrifugations at 14500 rpm for 20 min in a micro centrifuge Certomat IS Sartorius 5 µL of different NPs concentrations were added. The microtiter plates were incubated at 37ºC. The following step was made after 24 h, 48 h or 72 h. The content of the wells was removed and they were washed one time with PBS. Then, 100 µL of fresh medium and 10 µL of MTT 12 mM (Invitrogen) were added to each well. The plates were incubated at 37ºC for 30 min and when the blue crystals were formed the content of the wells was removed. After 10 min of incubation at room temperature the crystals were resuspended in 100 µL of DMSO (Sigma-Aldrich). Absorbance was read at 540 nm and 630 nm in a micro plate reader Infinite M200 Tecan.

3.8 Ecotoxicity of NPs

To evaluate the ecotoxicity of the NPs produced an assay with the algae *Dunaliella salina* was performed. *Dunaliella salina* (courtesy of Aquário Vasco da Gama) was maintained in filtered seawater, renewed every two days, with aeration and photoperiod at room temperature. *D. saline* growth curve was performed in seawater and measured by optical density reading at 680 nm (unpublished results of Miguel Larguinho). To evaluate the NPs ecotoxicity, the first step was to determine the number of algae in 1 mL of solution, for this objective 10 µL of algae was mixed with lugol (Sigma-Aldrich) in a 1:1 proportion and placed in a counting chamber that was observed with an optical microscope (Nikon TMS Japan, 0.2 A). 250 µL of algae suspension were added to a 24-well microtiter plate and then different concentrations of NPs were also added. To make up to a final volume of 500 µL, filtered seawater was added. The plates were left at room temperature with photoperiod. After 24 h or 48 h the algae of each well were counted. Duplicate determinations were performed for each of the three independent experiments.

Chapter 4 – Results

4.1 Characterisation of NPs

Five types of noble-metal NPs were synthesised via citrate co-reduction using an adaption of the Turkevich method [22,26]. One type was composed of only one metal, silver, while the other four types were silver:gold-alloys with different ratios. Apart from producing NPs with different compositions, to produce NPs with different sizes, different concentrations of citrate were used. The NPs were characterised by UV-Vis., ICP, and TEM.

The elemental composition of the five types of NPs produced is described according to the ICP results (Table 2).

Table 2 Elemental analysis of the five types of NPs produced

					Total amount of metal	
NPs Type	**Ag (mg/L)**	**Au (mg/L)**	**Ag %**	**Au %**	**(mM)**	**(mg/L)**
1	24.8	0	100	0	13	127.7
2	16.0	7.2	80	20	10	103.0
3	6.0	5.9	65	35	472	47.2
4	8.6	10.0	61	39	724	72.4
5	5.7	9.1	53	47	547	54.7

ICP analysis was also performed in the supernatant of the NPs produced to evaluate the presence of Ag^+ ions in solution. None of this analysis showed silver ions in solution above the detection limit of the method.

Although the initial amount of Ag and Au was the same for types 4 and 5 (Table 1), the ICP results demonstrated a difference in Ag:Au ratio and in the total amount of metal (Table 2).

Based on this analysis these NPs are designated in the remaining of this dissertation as shown in Table 3.

Table 3 NPs identification

NPs type	NPs identification
1	100% Ag NPs 38.8 mM citrate
2	80% Ag:20% Au NPs 38.8 mM citrate
3	65% Ag:35% Au NPs 38.8 mM citrate
4	61% Ag:39% Au NPs 34 mM citrate
5	53% Ag:47% Au NPs 34 mM citrate

A UV-Vis. analysis of the three batches synthesised for 100% Ag NPs 38.8mM citrate type was made in a spectrophotometer Uvmini-1240 Shimadzu (Fig. 4). For batches 04.04.13 and 09.04.13 at flask surface and bottom a UV-Vis. analysis was made separately because a colour difference was observed (Fig. 4).

In Fig. 4 it can be seen that the maximum wavelength does not vary more that 13 nm, between 402-415 nm, therefore, the three batches were pooled together. The same was made with the other NPs types.

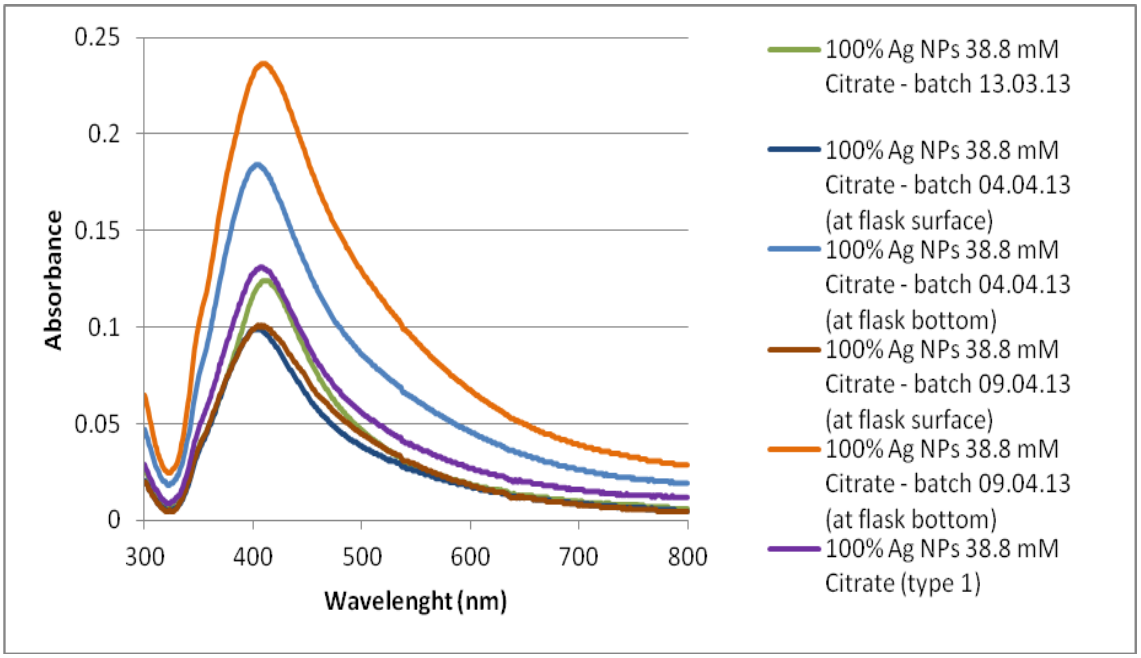

Fig. 4 UV-Vis. spectra of three produced batches of 100% Ag NPs 38.8 mM citrate

The five NPs types were characterised using UV-Vis. spectrophotometry in a Uvmini-1240 Shimadzu. Fig. 5 shows the NPs absorbance after 1:10 dilution in water.

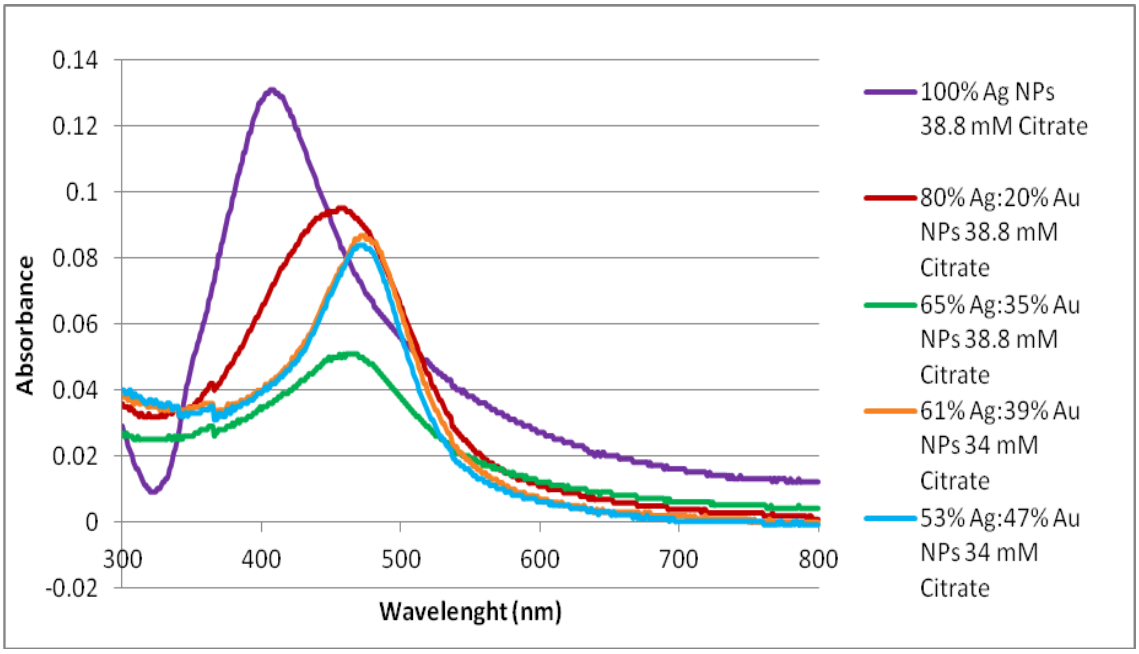

Fig. 5 UV-Vis. spectra of the five types of NPs produced

The reduction of Ag fraction in the composition of the NPs shifts the peak of maximum absorbance to the right (Fig. 5). This is summarised in Table 4.

Table 4 Maximum absorbance of NPs and the correspondent wavelength

NPs type	Maximum Absorbance	Wavelenght (nm)
100% Ag NPs 38.8 mM citrate	0.131	406-409
80% Ag:20% Au NPs 38.8 mM citrate	0.095	455-460
65% Ag:35% Au NPs 38.8 mM citrate	0.051	461-469
61% Ag:39% Au NPs 34 mM citrate	0.087	471-474
53% Ag:47% Au NPs 34 mM citrate	0.084	469-474

TEM analysis enables the determination of the average size and median of a set of NPs and their size distribution. NPs types presented mainly spherical shaped NPs. However 100% Ag NPs 38.8 mM citrate presented different shapes of NPs (Fig. 6). As such, the distribution of different particle shapes for 100% Ag NPs 38.8 mM citrate is presented in Table 5.

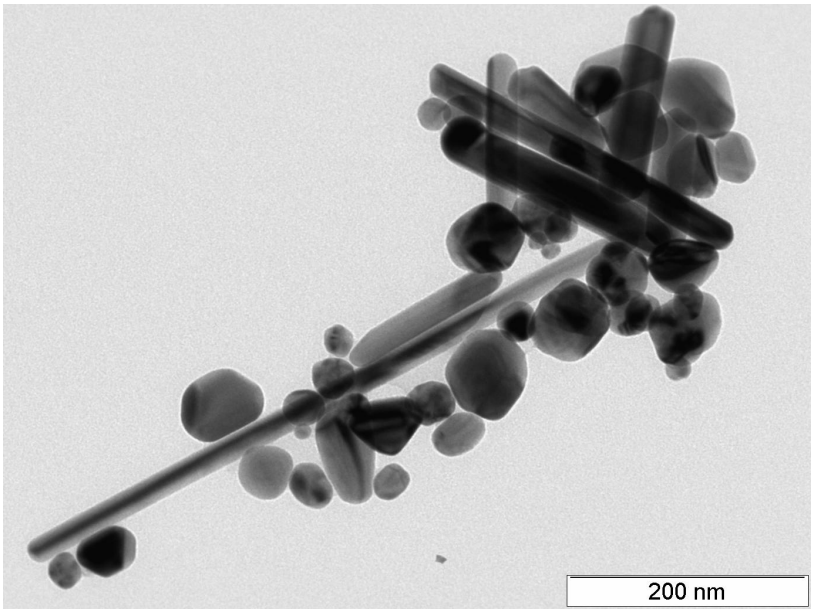

Fig. 6 TEM image of 100% Ag NPs 38.8 mM citrate

Table 5 Distribution of particles shapes of 100% Ag NPs 38.8 mM citrate

Needles/Rods	Triangles	Squares	Spheres	Total NPs
111	31	19	147	308
36%	10%	6%	48%	100%

The spherical 100% Ag NPs 38.8 Mm citrate have an average size of 40 nm and a median size of 38 nm (Table 6) and a size distribution with the higher count number of NPs between 18 nm and 64 nm (Fig. 7).

Table 6 Average size and median size of 100% Ag NPs 38.8 mM citrate

n	Average size (nm)	Median size (nm)
147	40±16	38

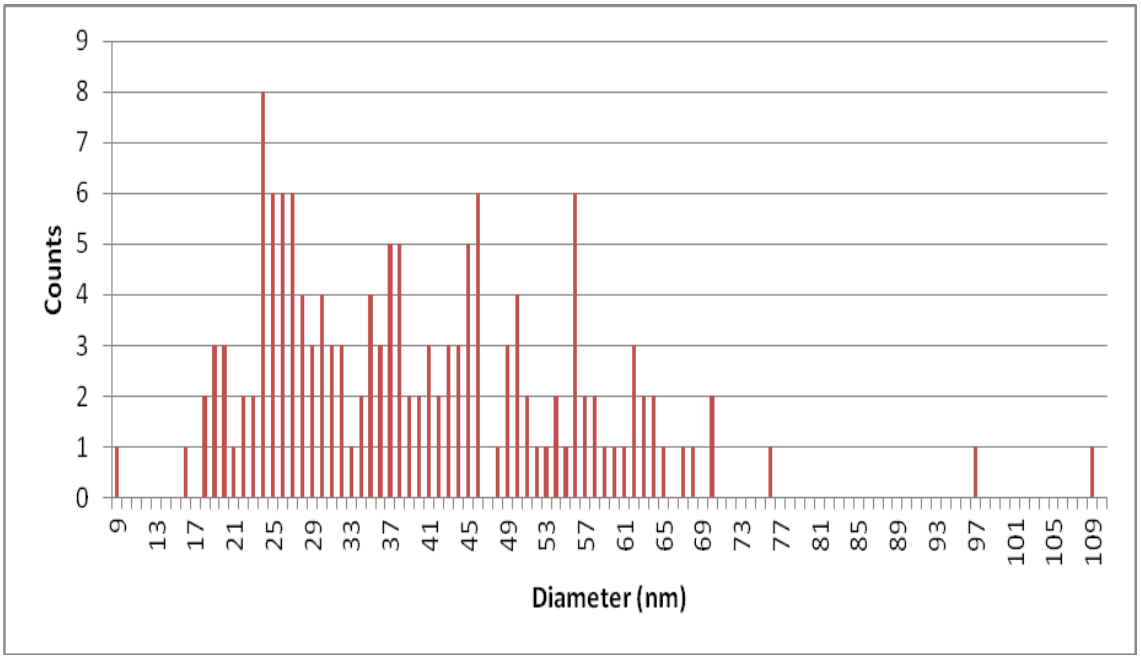

Fig. 7 Size distribution of 100% Ag NPs 38.8 mM citrate by TEM analysis

The average size of 80% Ag:20% Au NPs 38.8 mM citrate is 33 nm and the median size is 31 nm (Table 7) and their size distribution is primarily between 12 nm and 50 nm (Fig. 8). 80% Ag:20% Au NPs 38.8 mM citrate are mainly spherical shaped (Fig. 9).

Table 7 Average size and median size of 80% Ag:20% Au NPs 38.8 mM citrate

n	Average size (nm)	Median size (nm)
253	33±13	31

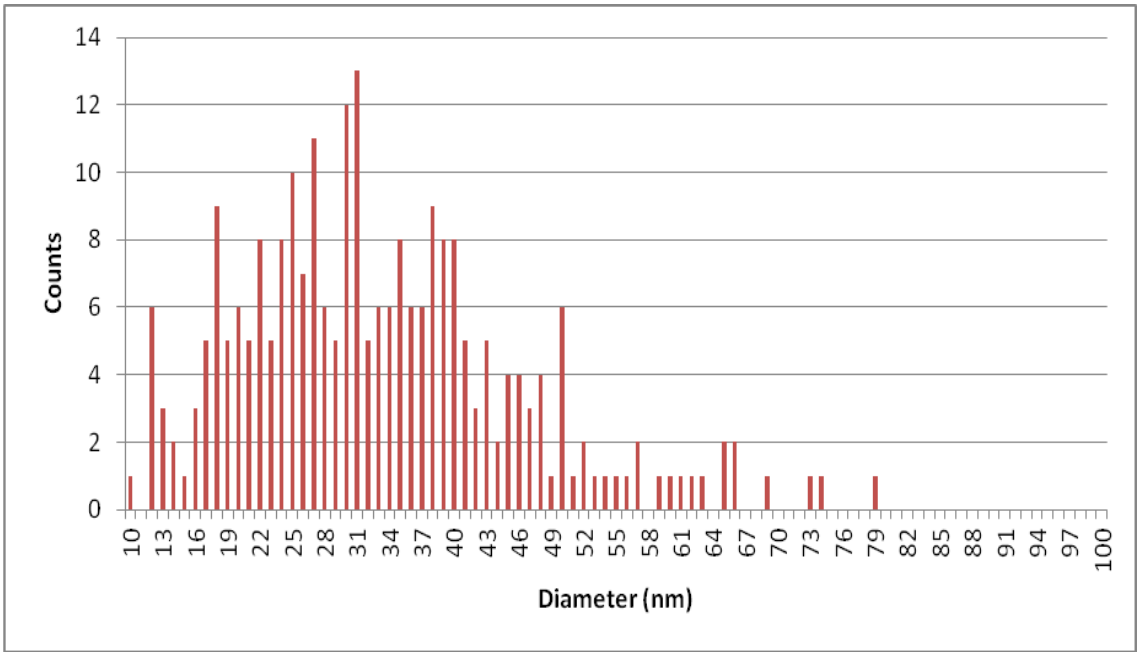

Fig. 8 Size distribution of 80% Ag:20% Au NPs 38.8 mM citrate by TEM analysis

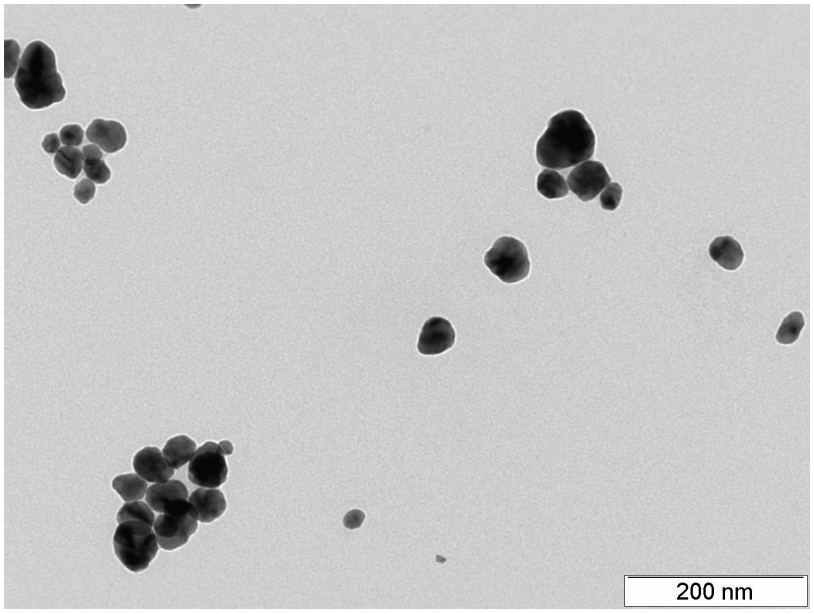

Fig. 9 TEM image of 80% Ag:20% Au NPs 38.8 mM citrate

The average size of 65% Ag:35% Au NPs 38.8 mM citrate is 48 nm and the median size is 51 nm (Table 8) and their size distribution is primarily between 20 nm and 72 nm (Fig. 10). 65% Ag:35% Au NPs 38.8 mM citrate are mostly spherical shaped (Fig. 11).

Table 8 Average size and median size of 65% Ag:35% Au NPs 38.8 mM citrate

n	Average size (nm)	Median size (nm)
593	48±14	51

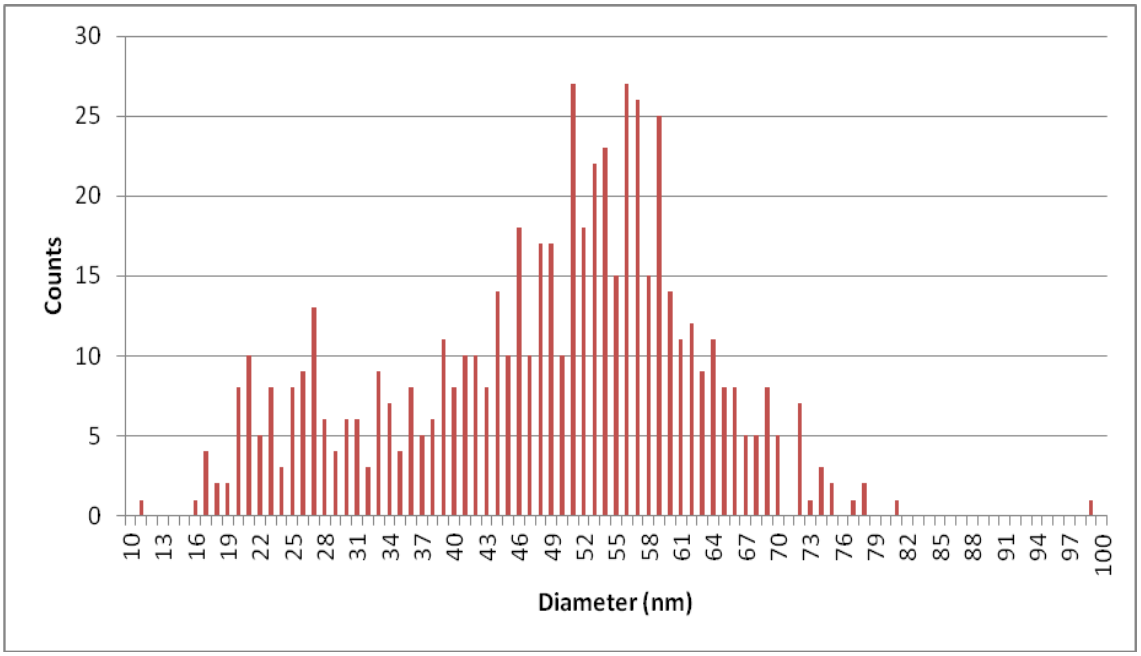

Fig. 10 Size distribution of 65% Ag:35% Au NPs 38.8 mM citrate by TEM analysis

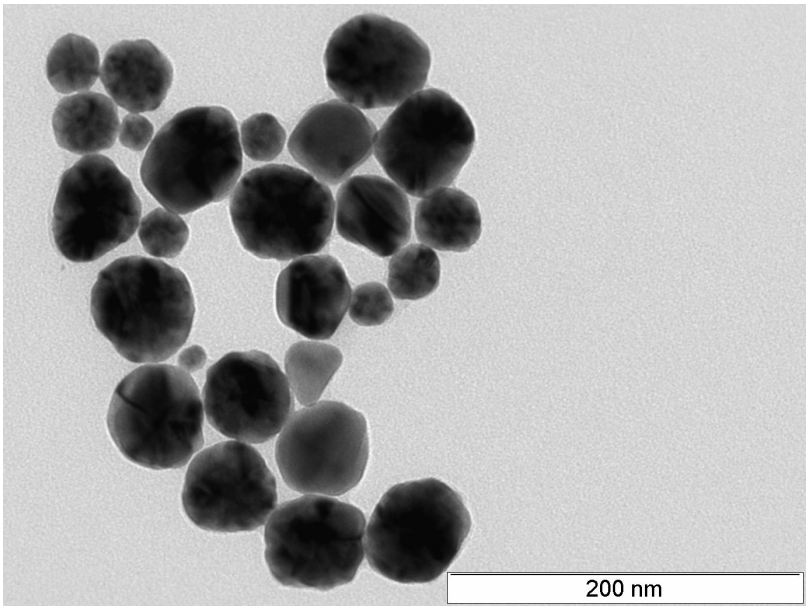

Fig. 11 TEM image of 65% Ag:35% Au NPs 38.8 mM citrate

The 61% Ag:39% Au NPs 34 mM citrate have a size distribution with the higher count number of NPs between 10 nm and 23 nm and between from 42 nm until 75 nm (Fig. 12). 61% Ag:39% Au NPs 34 mM citrate are principally spherical shaped and clearly present two distinct size ranges (Fig. 13).

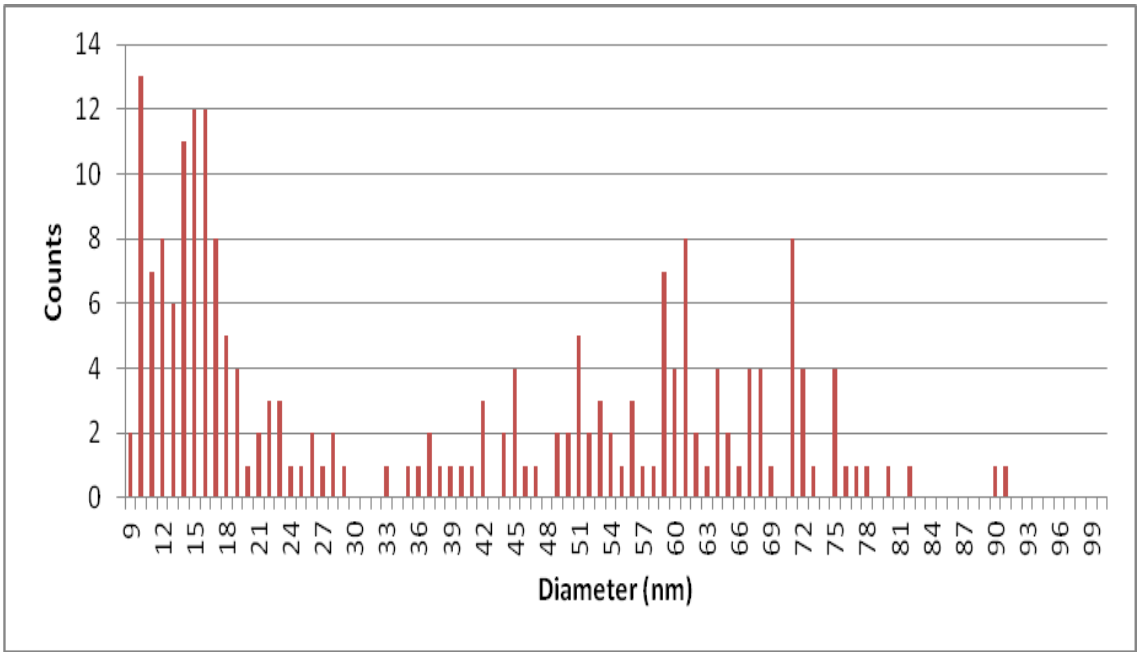

Fig. 12 Size distribution of 61% Ag:39% Au NPs 34 mM citrate by TEM analysis

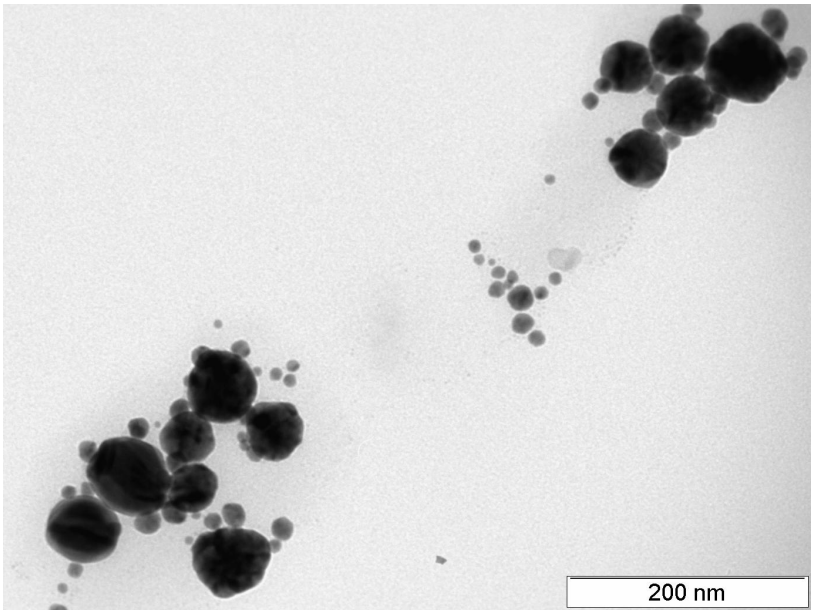

Fig. 13 TEM image of 61% Ag:39% Au NPs 34 mM citrate

61% Ag:39% Au NPs 34 mM citrate have two different distribution size groups. NPs between 10 nm and 23 nm have an average size of 16 nm and a median size of 15 nm (Table 9). NPs between 42 nm and 75 nm have an average size of 59 nm and median size of 60 nm (Table 10).

Table 9 Average size and median size of 61% Ag:39% Au NPs 34 mM citrate between 9 nm and 30 nm

n	Average size (nm)	Median size (nm)
105	16±6	15

Table 10 Average size and median size of 61% Ag:39% Au NPs 34 mM citrate between 31 nm and 91 nm

n	Average size (nm)	Median size (nm)
104	59±18	60

The average size of 53% Ag:47% Au NPs 34 mM citrate is 51 nm and the median size is 53 nm (Table 11). Their size distribution is primarily between 38 nm and 66 nm (Fig. 14). 53% Ag:47% Au NPs 34 mM citrate are above all spherical shaped (Fig. 15).

Table 11 Average size and median size of 53% Ag:47% Au NPs 34 mM citrate

n	Average size (nm)	Median size (nm)
466	51±11	53

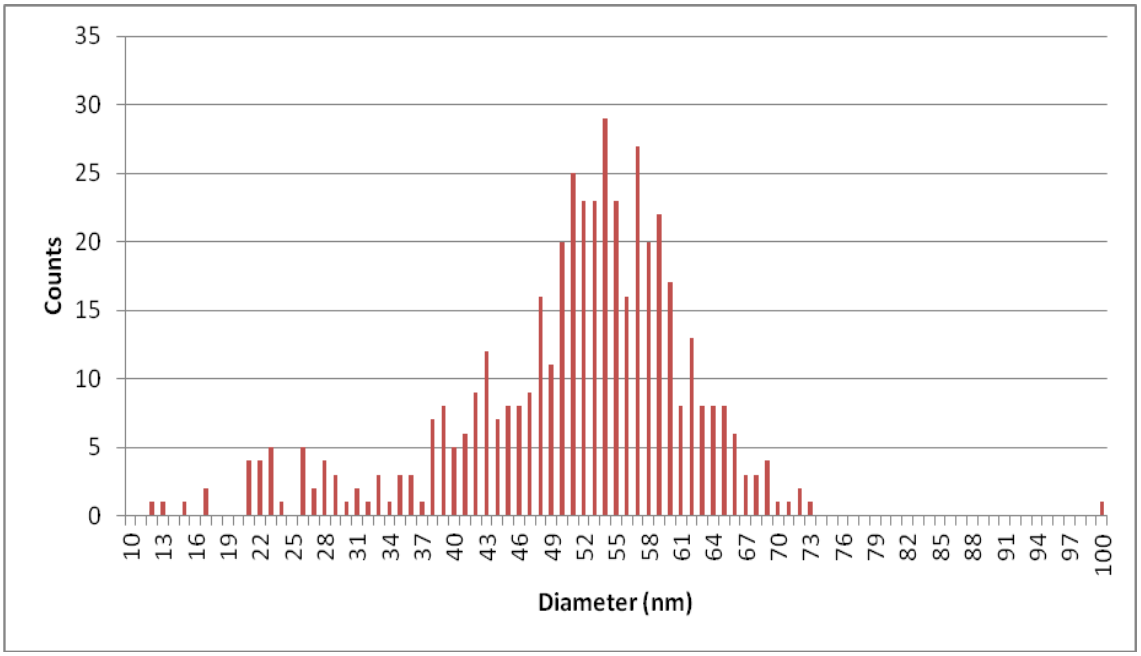

Fig. 14 Size distribution of 53% Ag:47% Au NPs 34 mM citrate by TEM analysis

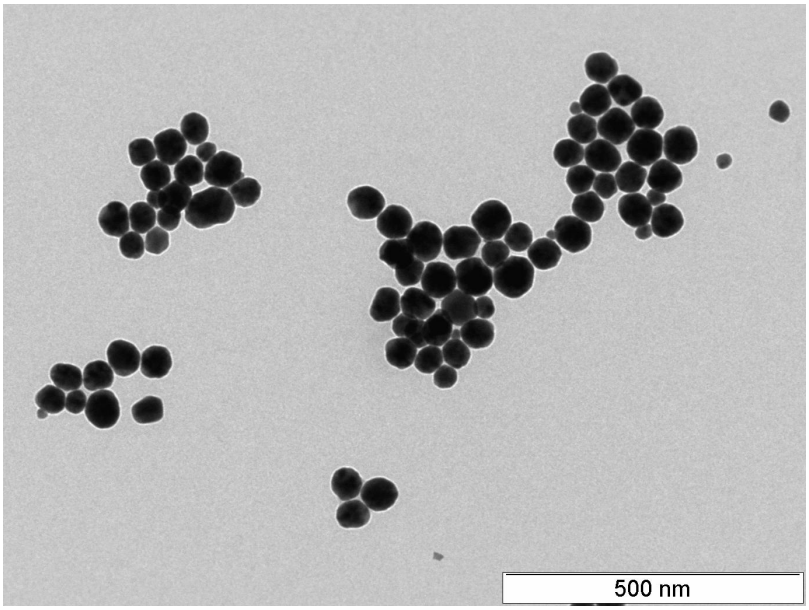

Fig. 15 TEM image of 53% Ag:47% Au NPs 34 mM citrate

With the exception of 61% Ag:39% Au NPs 34 mM citrate that have two different size range groups, the other particles have a size variation between 33±13 nm and 51±11 nm (Table 12).

Table 12 Median size and average size of NPs types

NPs type	n	Median size (nm)	Average size (nm)
100% Ag NPs 38.8 mM citrate	147	38	40±16
80% Ag:20% Au NPs 38.8 mM citrate	253	31	33±13
65% Ag:35% Au NPs 38.8 mM citrate	593	51	48±14
61% Ag:39% Au NPs 34 mM citrate (from 9 nm to 30 nm)	105	15	16±6
61% Ag:39% Au NPs 34 mM citrate (from 31 nm to 91 nm)	104	60	59±18
53% Ag:47% Au NPs 34 mM citrate	466	53	51±11

To evaluate the stability of the produced NPs, they were added to the different grow media that were used along the experiments and incubated at 37ºC. UV-Vis. spectra were measured in a micro plate reader Infinite M200 Tecan after different times.

Spectra of NPs were analysed in water to demonstrate their stability over time (Fig. 16). The concentration of the NPs was 33.75-fold the concentration indicated in Table 2. The results illustrated in Fig. 16 were obtained for 65% Ag:35% Au NPs 38.8 mM citrate which have a maximum absorbance at 468 nm for the different time points. This wavelength value is within the range previously observed for this NPs type (Table 4). Stability of the other produced NPs along time in water was also observed, with wavelength values within the expected range showed in Table 4 (data not shown).

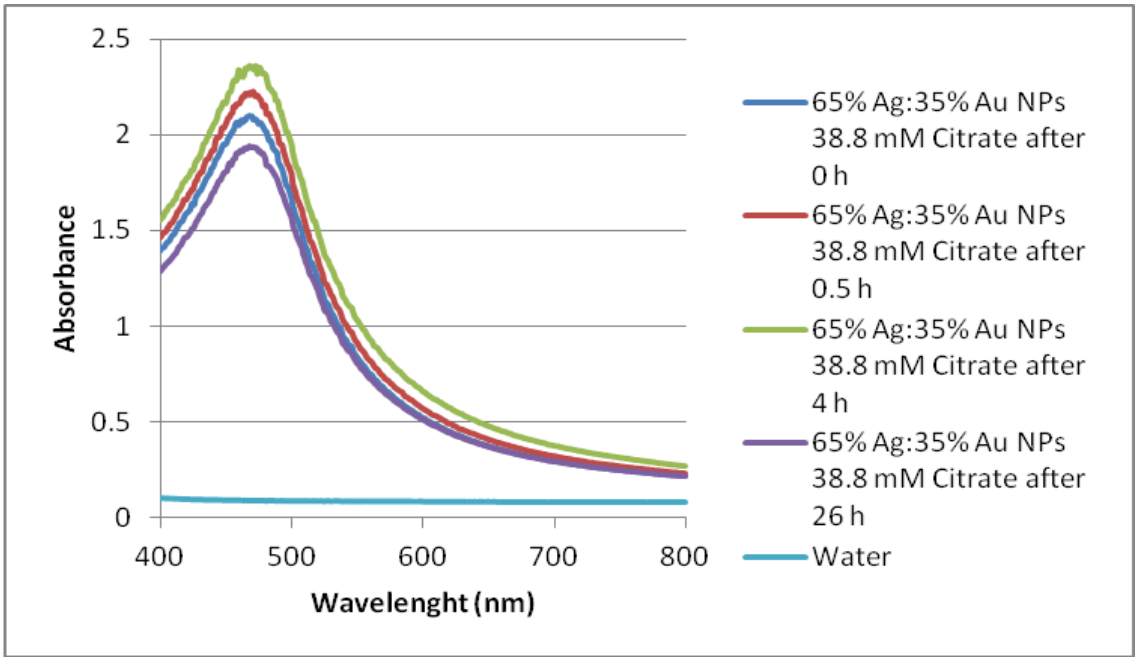

Fig. 16 UV-Vis. spectra of 65% Ag:35% Au NPs 38.8 mM citrate in water after 0 h, 0.5 h, 4 h and 26 h of incubation at 37ºC

Stability of NPs in LB medium was also evaluated (Fig. 17, Fig. 18, Fig. 19 and Fig. 20). The concentration of the NPs was 33.75-fold the concentration indicated in Table 2.

100% Ag NPs 38.8 mM citrate aggregated between 4 h and 26 h (Fig. 17). All the alloy-NPs lose their stability between 0.5 h and 4 h (Fig. 18, Fig. 19 and Fig. 20). However it can be observed that some NPs might already started to aggregate at zero time (Fig. 17, Fig. 18, Fig. 19 and Fig. 20).

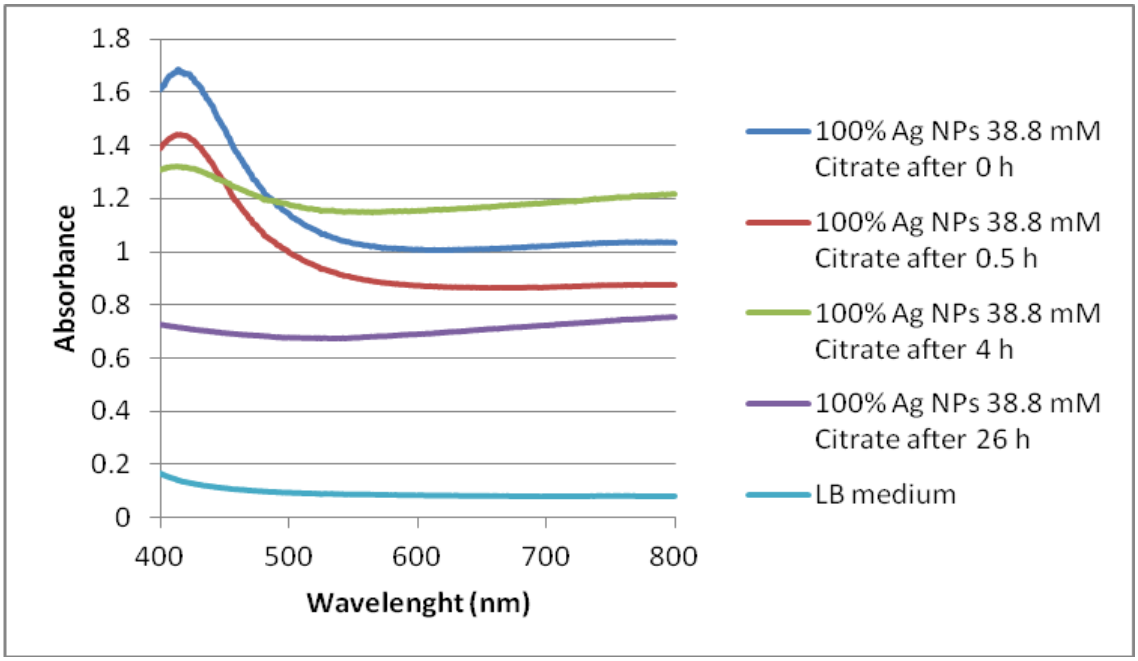

Fig. 17 UV-Vis. spectra of 100% Ag NPs 38.8 mM citrate after 0 h, 0.5 h, 4 h and 26 h of incubation in LB

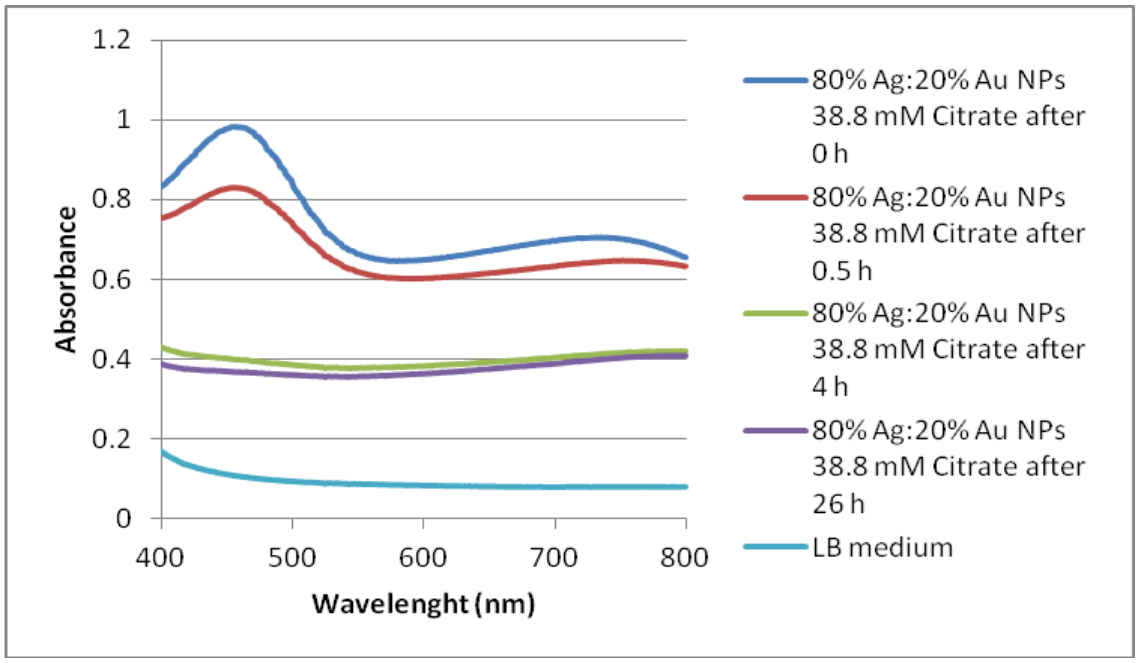

Fig. 18 UV-Vis. spectra of 80% Ag:20% Au NPs 38.8 mM citrate after 0 h, 0.5 h, 4 h and 26 h of incubation in LB

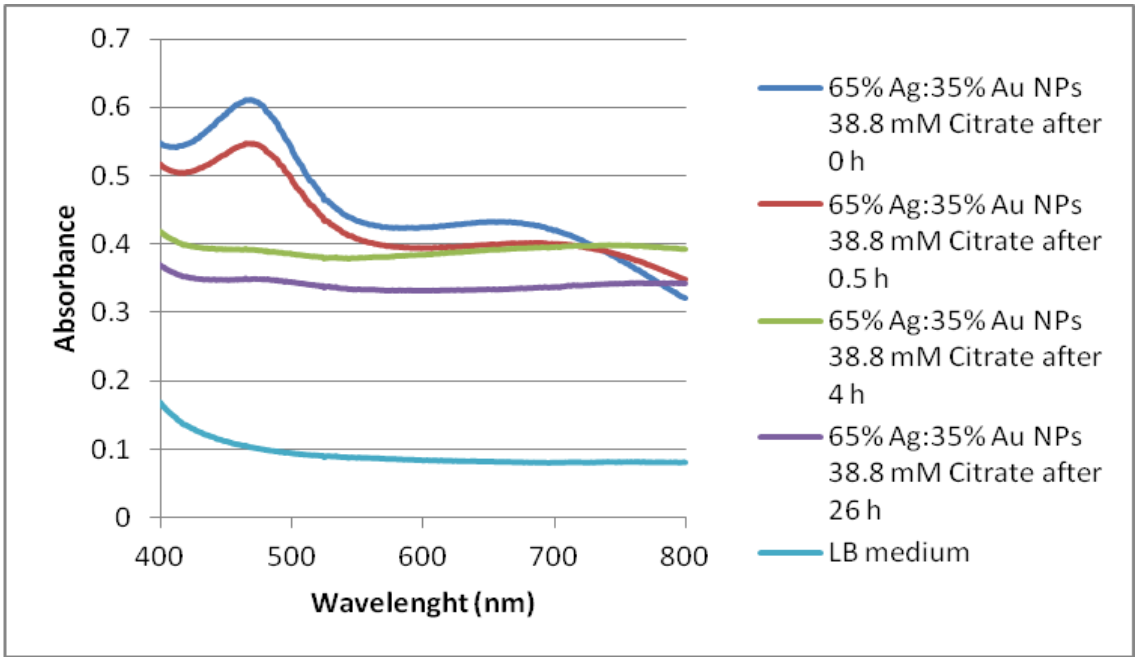

Fig. 19 UV-Vis. spectra of 65% Ag:35% Au NPs 38.8 mM citrate after 0 h, 0.5 h, 4 h and 26 h of incubation in LB

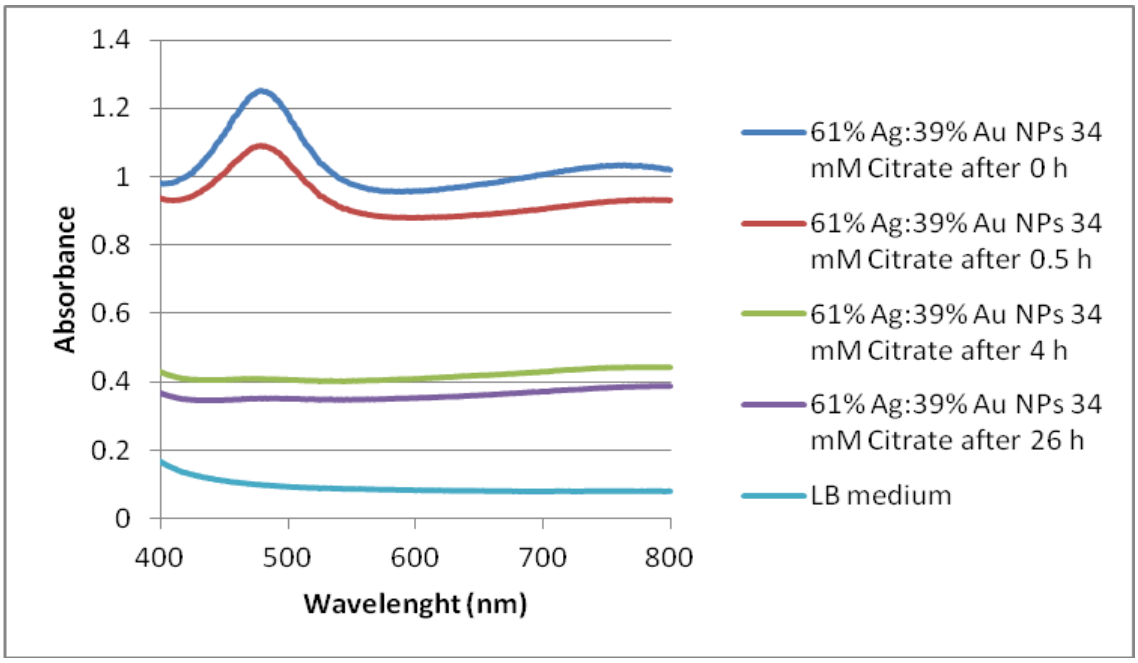

Fig. 20 UV-Vis. spectra of 61% Ag:39% Au NPs 34 mM citrate after 0 h, 0.5 h, 4 h and 26 h of incubation in LB

Stability of NPs in TSB medium was also evaluated (Fig. 21, Fig. 22, Fig. 23 and Fig. 24). The concentration of the NPs was 33.75-fold the concentration indicated in Table 2.

100% Ag NPs 38.8 mM citrate, 80% Ag:20% Au NPs 38.8 mM citrate and 61% Ag:39% Au NPs 34 mM citrate aggregated between 4 h and 26 h (Fig. 21, Fig. 22 and Fig. 24). The 65% Ag:35% Au NPs 38.8 mM citrate aggregated after 26h (Fig. 23). Yet it can be observed that the aggregation started after time zero (Fig. 21, Fig. 22, Fig. 23 and Fig. 24).

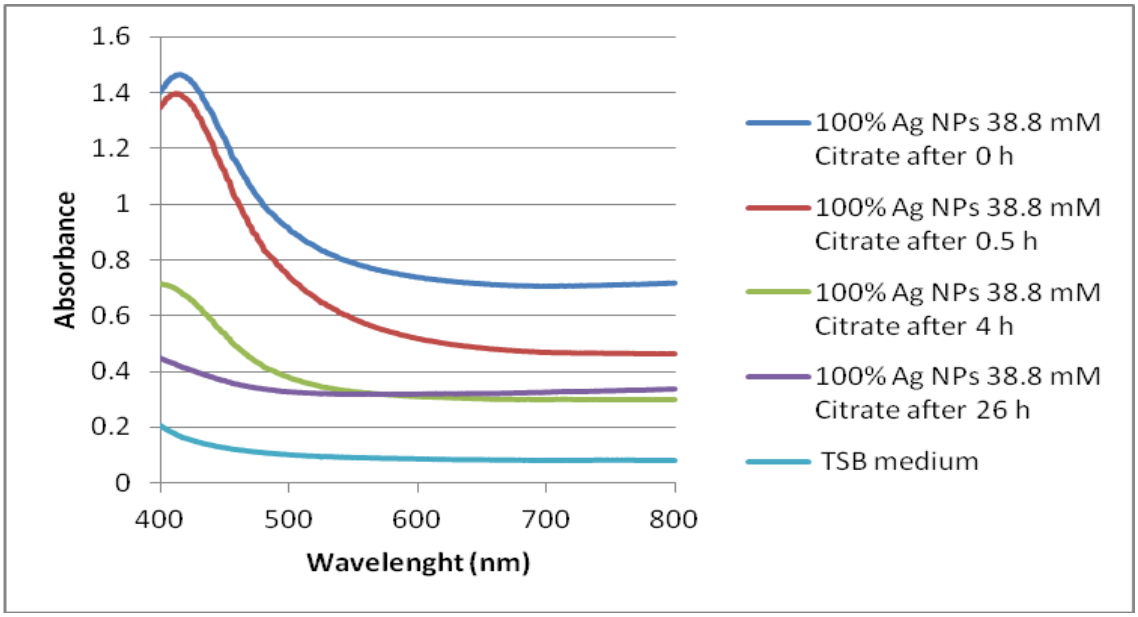

Fig. 21 UV-Vis. spectra of 100% Ag NPs 38.8 mM citrate after 0 h, 0.5 h, 4 h and 26 h of incubation in TSB

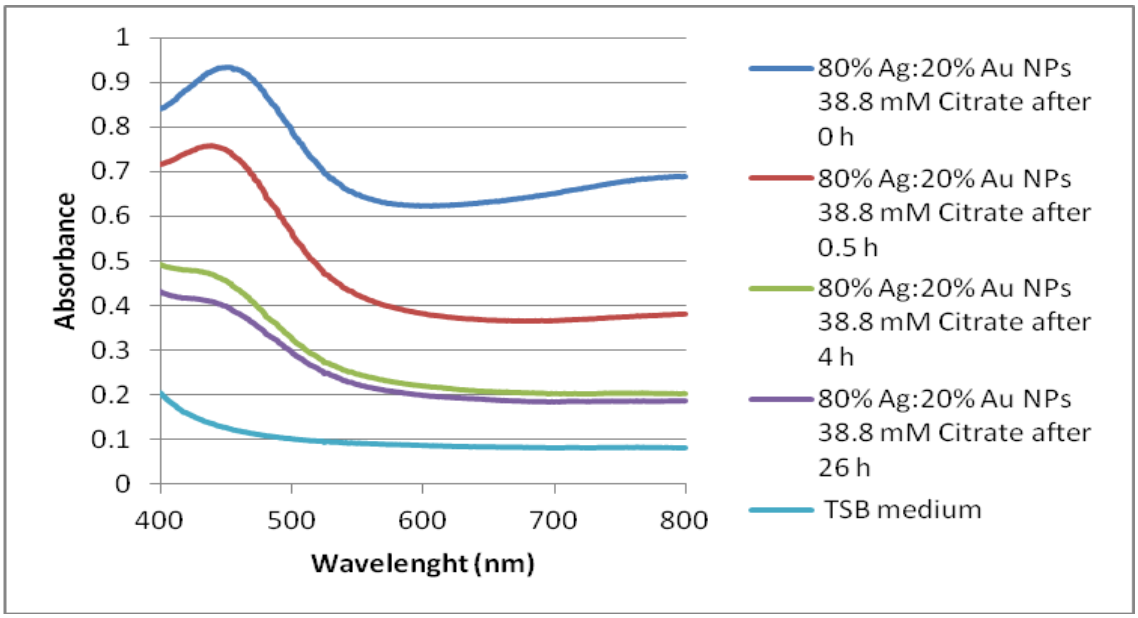

Fig. 22 UV-Vis. spectra of 80% Ag:20% Au NPs 38.8 mM citrate after 0 h, 0.5 h, 4 h and 26 h of incubation in TSB

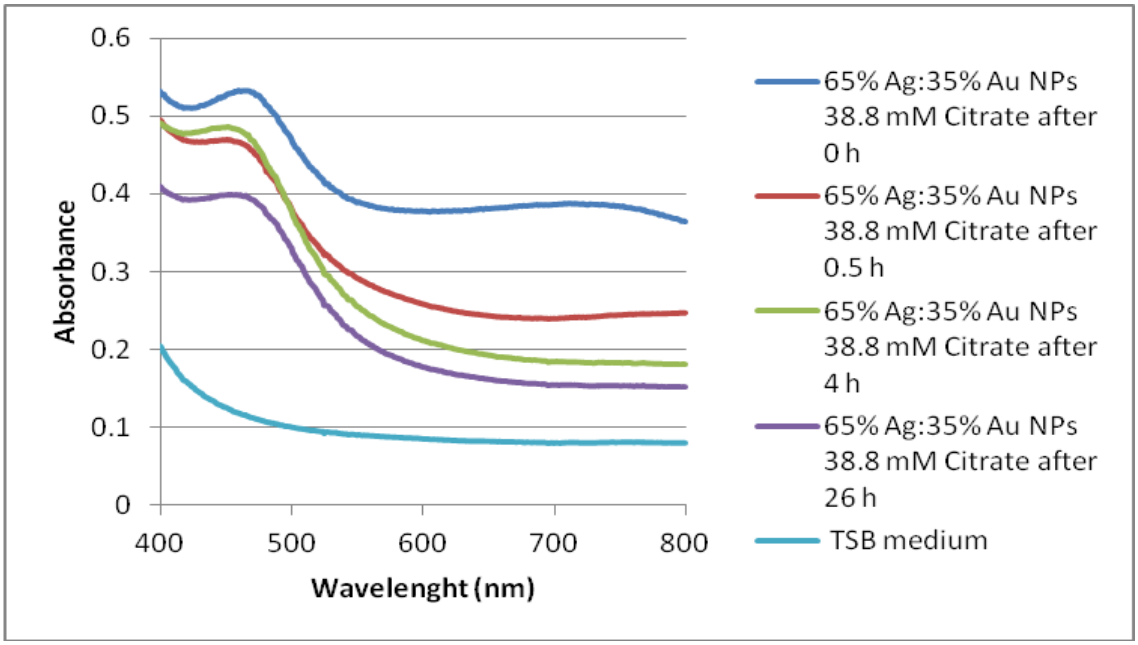

Fig. 23 UV-Vis. spectra of 65% Ag:35% Au NPs 38.8 mM citrate after 0 h, 0.5 h, 4 h and 26 h of incubation in TSB

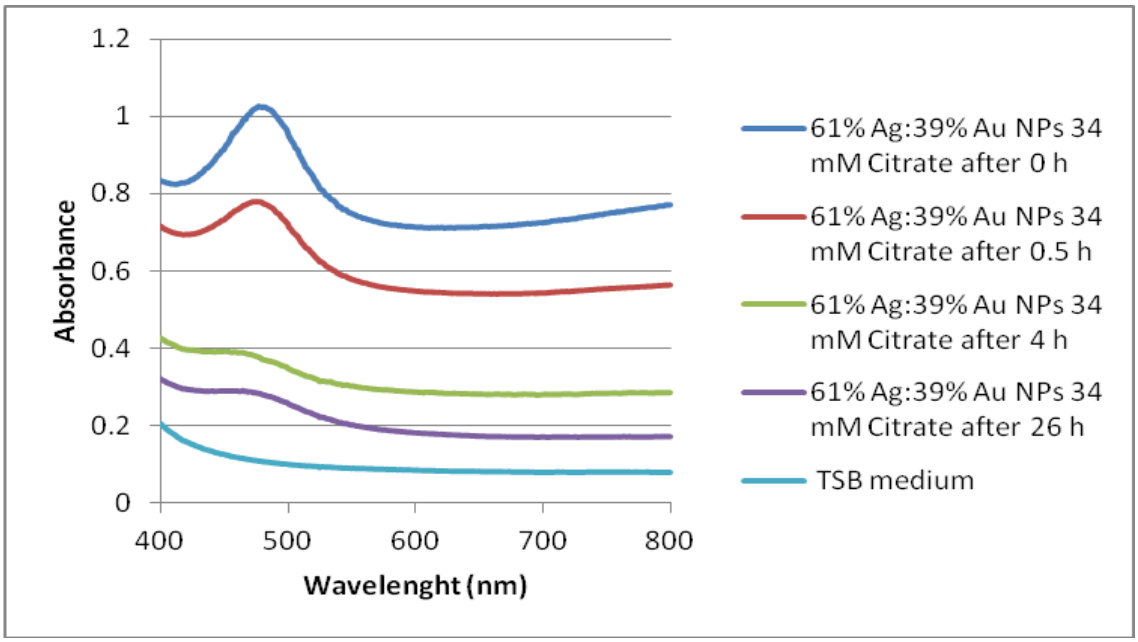

Fig. 24 UV-Vis. spectra of 61% Ag:39% Au NPs 34 mM citrate after 0 h, 0.5 h, 4 h and 26 h of incubation in TSB

Stability of NPs in DMEM medium was also evaluated (Fig. 25, Fig. 26, Fig. 27 and Fig. 28). The NPs had a total amount of 541 mg/mL of Ag.

80% Ag:20% Au NPs 38.8 mM citrate seem to be aggregated from time zero on (Fig. 26) All the other NPs showed less aggregation, however, they all began to lose their stability from time zero (Fig. 25, Fig. 27 and Fig. 28).

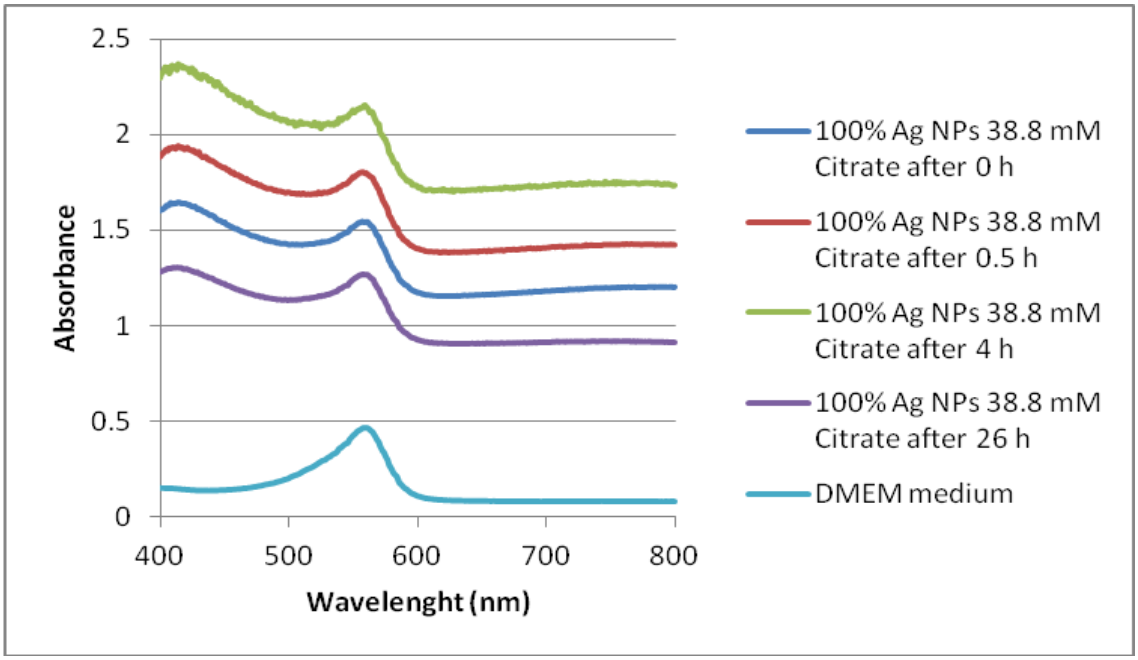

Fig. 25 UV-Vis. spectra of 100% Ag NPs 38.8 mM citrate after 0 h, 0.5 h, 4 h and 26 h of incubation in DMEM

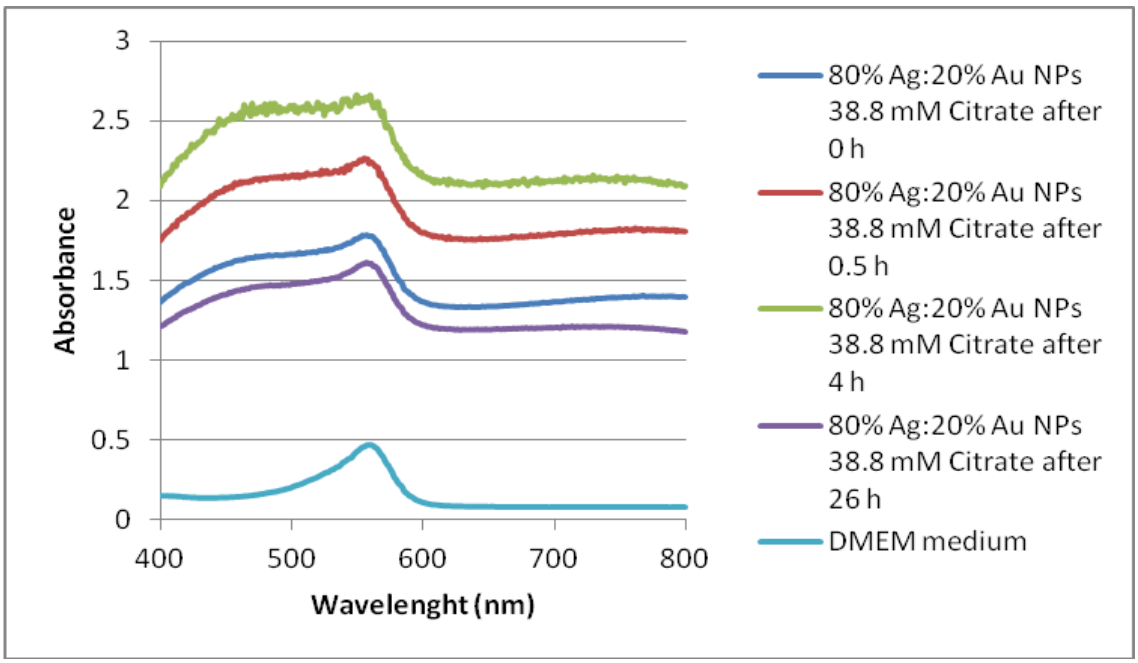

Fig. 26 UV-Vis. spectra of 80% Ag:20% Au NPs 38.8 mM citrate after 0 h, 0.5 h, 4 h and 26 h of incubation in DMEM

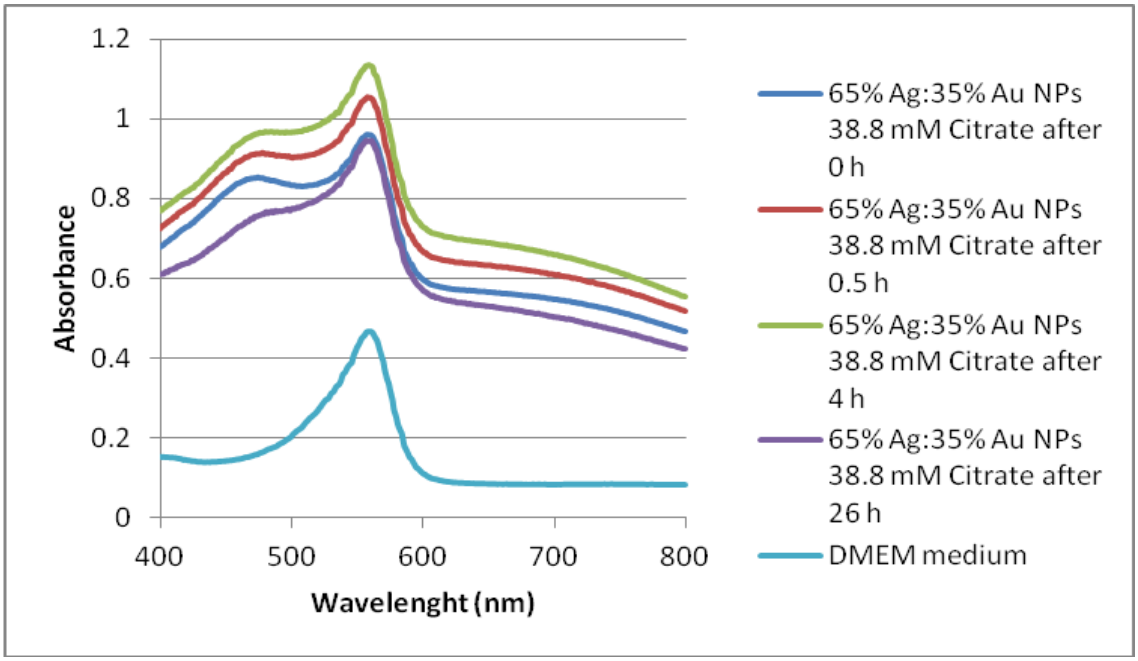

Fig. 27 UV-Vis. spectra of 65% Ag:35% Au NPs 38.8 mM citrate after 0 h, 0.5 h, 4 h and 26 h of incubation in DMEM

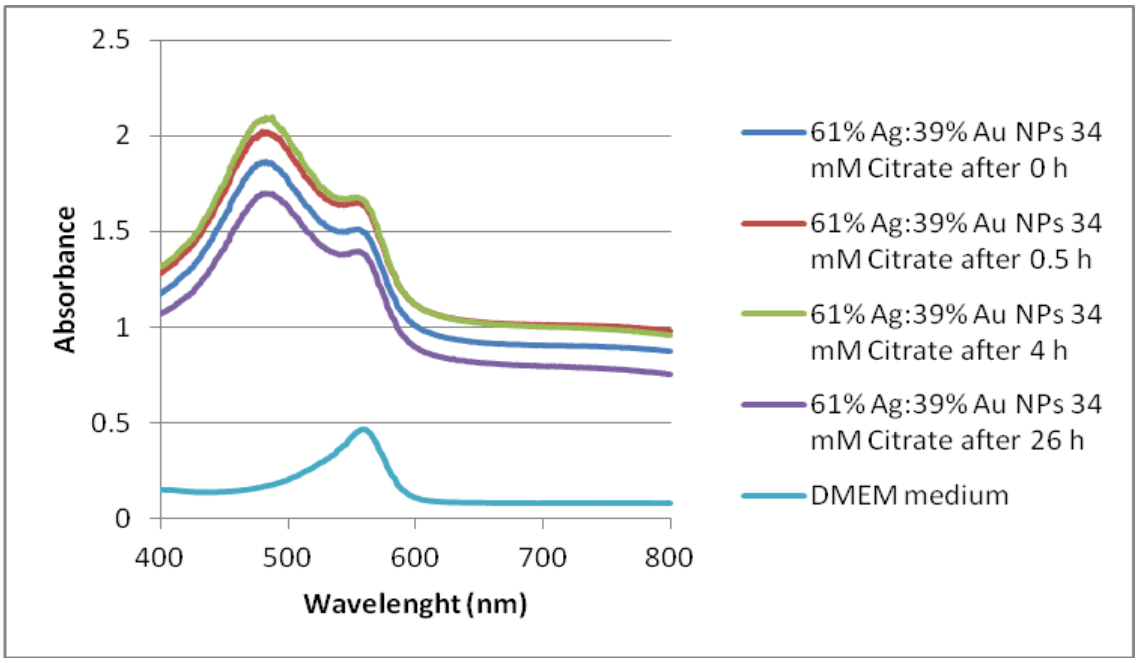

Fig. 28 UV-Vis. spectra of 61% Ag:39% Au NPs 34 mM citrate after 0 h, 0.5 h, 4 h and 26 h of incubation in DMEM

Stability of NPs in seawater was also evaluated (Fig. 29). The NPs had a total amount of 1 mg/mL of Ag.

In Fig. 29 is possible to observe that 61% Ag:39% Au NPs 34 mM citrate are almost aggregated to a long extent from time zero. Complete aggregation of other produced NPs in seawater was also observed from time zero (data not shown).

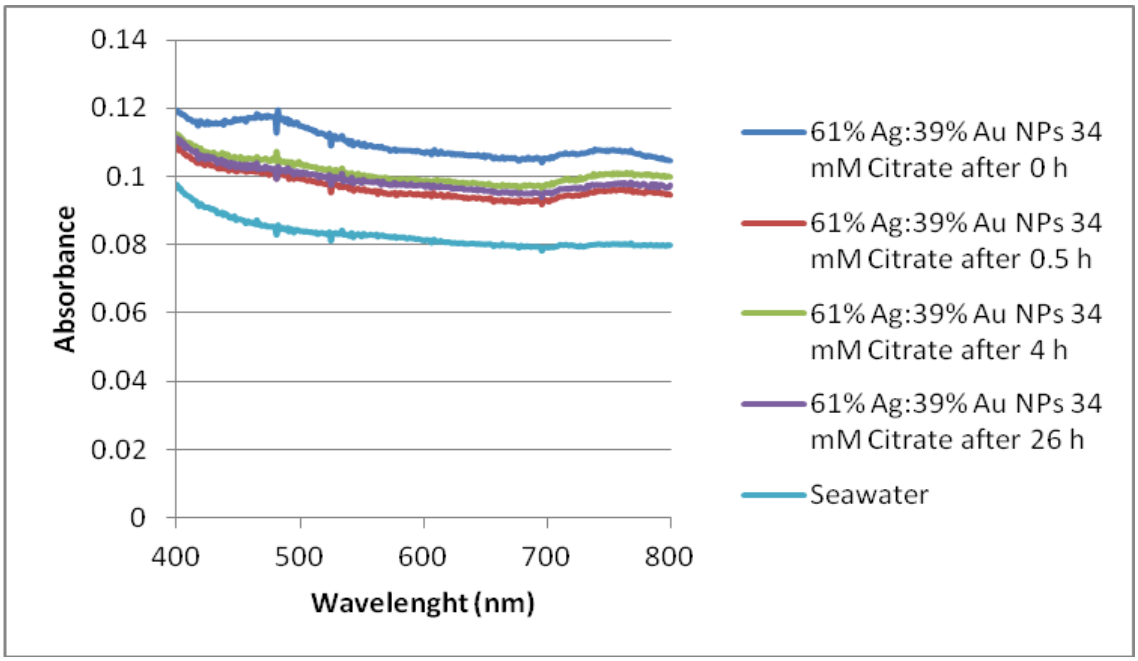

Fig. 29 UV-Vis. spectra of 61% Ag:39% Au NPs 34 mM citrate after 0 h, 0.5 h, 4 h and 26 h of incubation in seawater

4.2 Characterisation of Biofilms

4.2.1 On microscope slides

To evaluate the ability of biofilm formation on glass, cells were incubated in liquid media in a Petri dish containing a glass slide in the bottom, for different time periods.

Microscopic analysis of slides reveals that biofilm of *S. aureus* is more quickly formed, in about 8 days, and 4 days later reaches a high cell density. *E. coli* biofilm is formed in about 24 days (Table 13).

After 30 days of incubation for *E. coli* and 35 days for *S. aureus* the cell density suffers a great decrease (Table 13).

Table 13 Microscopic analysis of *E. coli* and *S. aureus* biofilm formation

	Time (days)	Number of cells	Distribution pattern	Clusters and gaps
E. coli	8	**-**	Random in a single plane	**-**
	14	**-**	Random in a single plane	**-**
	24	**+**	Random in different planes	**+**
	30	**0**	None	**0**
S. aureus	8	**+**	Irregular in different planes	**+**
	12	**+ +**	Irregular in different planes	**+**
	13	**+ +**	Irregular in different planes	**+**
	24	**+ +**	Irregular in different planes	**+**
	35	**-**	Random in a single plane	**+**

Label:

0	None
-	Few
+	Some
+ +	Many

Photos of *S. aureus*, in a microscopic slide, were taken after an incubation period of 15 days (Fig. 30, Fig. 31, Fig. 32 and Fig. 33).

In Fig. 30 to Fig. 33 biofilm might present some poorly defined structures such as clusters, and in Fig. 32 and Fig. 33 some gaps can be observed. Fig. 30 might present a structure that look like a channel.

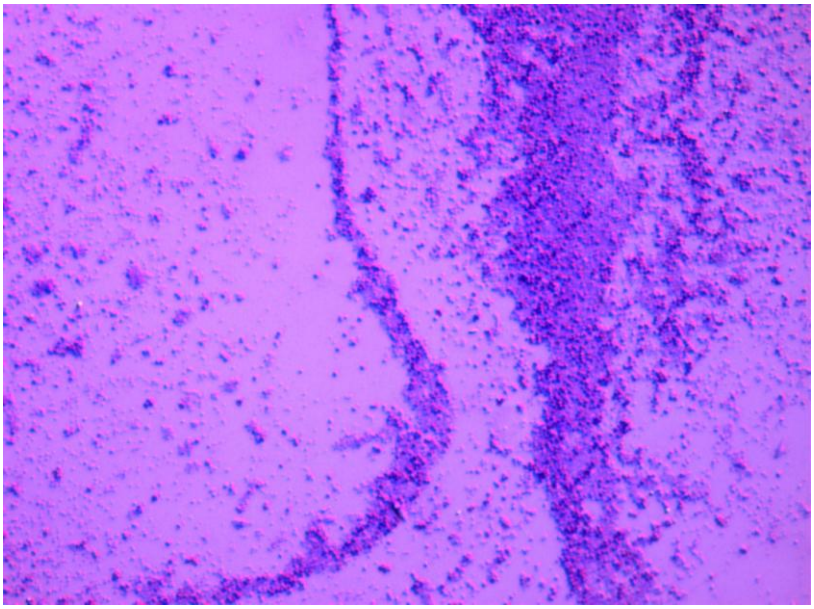

Fig. 30 Photo of *S. aureus* biofilm after 15 days of incubation

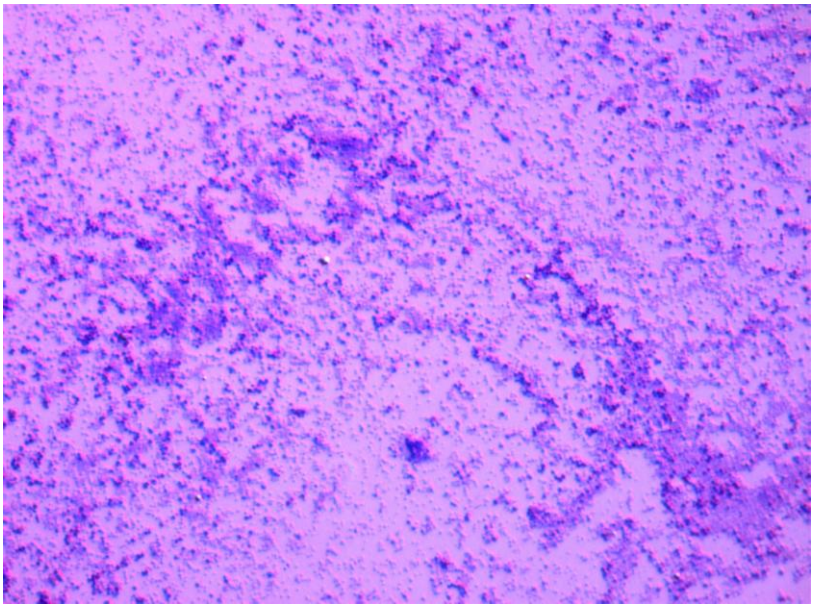

Fig. 31 Photo of *S. aureus* biofilm after 15 days of incubation

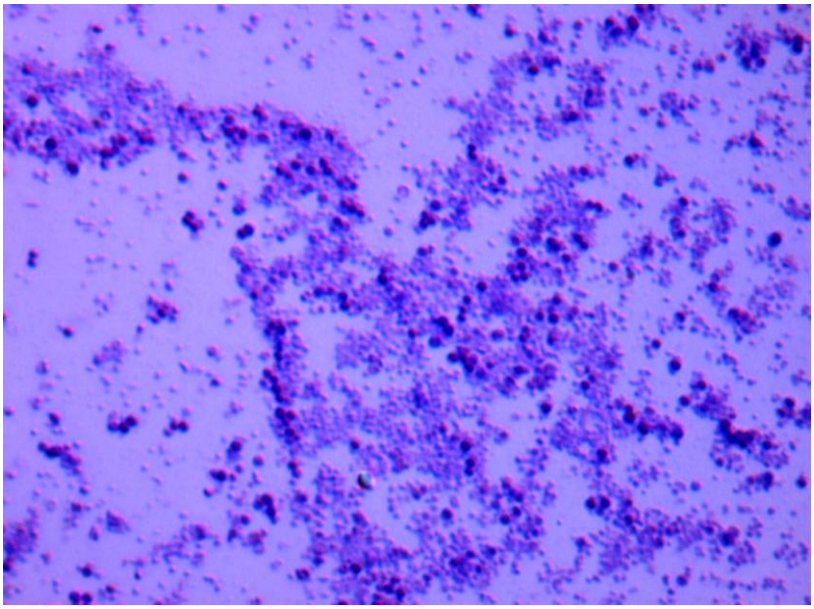

Fig. 32 Photo of *S. aureus* biofilm after 15 days of incubation

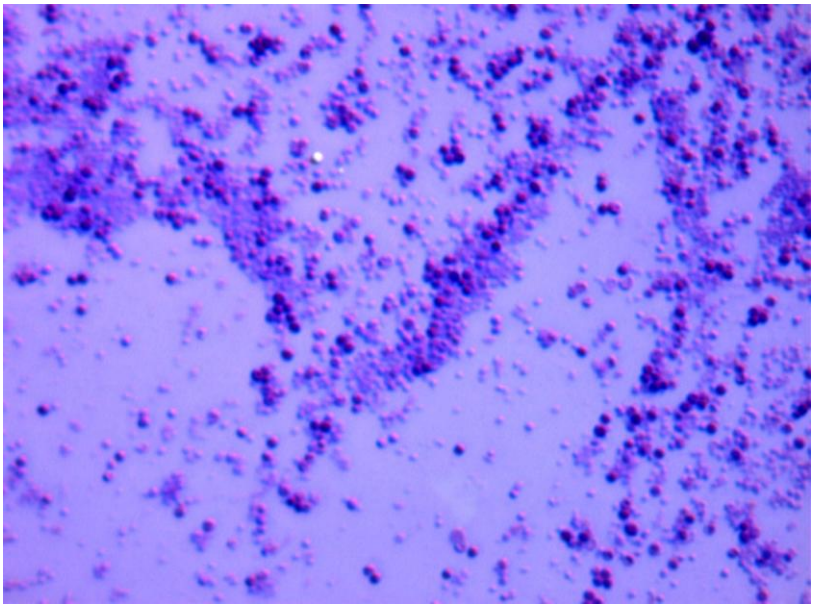

Fig. 33 Photo of *S. aureus* biofilm after 15 days of incubation

4.2.2 On microtiter plates

Biofilm formation of *E. coli* and *S. aureus* in liquid media was studied after a 24 h and 72 h of incubation at 37ºC in a 96-well microtiter plate.

The results were evaluated by UV-Vis. analysis enabling the measurement of biofilm formation by its adherence. The results indicate that this assay is more

qualitative, qualifying the biofilm formation by its adhesion force, than quantitative. In brief, the analysis is performed by an evaluation of optical density measurement, where obtained absorbance for one sample (ODc) is characterized by three standard deviations above the mean OD of the negative control (Table 14) [27].

Table 14 Quantitative analysis method for biofilm adherence

Analysis method	Biofilm adherence
OD ≤ ODc	non-adherence
ODc < OD ≤ 2x ODc	Weakly adherence
2x ODc < OD ≤ 4x ODc	Moderately adherence
4x ODc < OD	Strongly adherence

Table 15 shows that *E. coli* forms a strongly adherent biofilm at 24 h for 100% of the executed experiments and 70% at 72 h.

Table 15 Biofilm adherence of *E. coli*

E. coli **(n=10)**	**Biofilm adherence**		
	Weakly	**Moderately**	**Strongly**
24 h	0%	0%	100%
72 h	10%	20%	70%

Table 16 shows that *S. aureus* forms a strongly adherent biofilm at 24 h for 100% of the executed experiments, for 72 h results exhibit 73% frequency of strong biofilm adhesion.

Table 16 Biofilm adherence of *S. aureus*

S. aureus **(n=11)**	**Biofilm adherence**		
	Weakly	**Moderately**	**Strongly**
24 h	0%	0%	100%
72 h	9%	18%	73%

4.3 Biofilm growth inhibition in a 96-well microtiter plate

4.3.1 Inhibition of biofilm growth by antibiotic activity

Biofilm formation was also evaluated in the presence of antibiotics as the experiments in section 4.2.2. After MICs calculation, 0.1 mg/mL Kanamycin MIC was 2.35E-04 mg/mL and 0.5 mg/mL ampicillin MIC was 3.00E-04 mg/mL.

Table 17 summarises the Km activity for *E. coli*. After 24 h of incubation with MIC, the majority of cases evaluated correspond to a 56% frequency of weakly biofilm adhesion and after 72 h correspond to a 44% frequency of moderately biofilm adhesion. A strong biofilm adhesion can be observed for the experiments in which the amount of antibiotic used was above the MIC.

Table 17 Biofilm adherence of *E. coli* treated with Km

***E. coli* + Km (n=9)**		**Biofilm adherence**		
		Weakly	**Moderately**	**Strongly**
MIC	**24 h**	56%	44%	0%
	72 h	22%	44%	33%
50% MIC	**24 h**	0%	22%	78%
	72 h	0%	33%	67%
25% MIC	**24 h**	0%	22%	78%
	72 h	0%	44%	56%
0% MIC	**24 h**	0%	0%	100%
	72 h	11%	22%	67%

Table 18 shows the results for *S. aureus* treated with Amp, where 100% of the experiments with MIC, and 50% MIC after 24 h of incubation resulted in biofilms with weakly adhesion. After 72 h of incubation with MIC, 50% of the experiments resulted in biofilms with weakly adhesion and the other 50% in biofilms with moderately adhesion. 50% of experiments resulting in moderately biofilm adhesion and 50% in strongly biofilm adhesion is obtained after a 72 h of incubation with 50% MIC.

Table 18 Biofilm adherence of *S. aureus* treated with Amp

***S. aureus* + Amp (n=2)**		**Biofilm adherence**		
		Weakly	**Moderately**	**Strongly**
MIC	**24 h**	100%	0%	0%
	72 h	50%	50%	0%
50% MIC	**24 h**	100%	0%	0%
	72 h	0%	50%	50%
25% MIC	**24 h**	0%	0%	100%
	72 h	0%	0%	100%
0% MIC	**24 h**	0%	0%	100%
	72 h	0%	0%	100%

4.3.2 Inhibition of biofilm growth by NPs activity

Biofilm formation of *E. coli* and *S. aureus* was also evaluated in the presence of NPs (as performed in section 4.2.2). The concentration of the NPs was 33.75-fold the concentration indicated in Table 2.

After 24 h of incubation of *E. coli* with 100% Ag NPs 38.8 mM citrate and after 24 h and 72 h of incubation with 80% Ag:20% Au NPs 38.8 mM citrate, 100% of the experiments presented weakly adherent biofilm formation. Although for 100% Ag NPs 38.8 mM citrate after 72 h of incubation a frequency of 67% presented strongly adherent biofilm formation. 65% Ag:35% Au NPs 38.8 mM citrate have 100% frequency of experiments resulting in strongly adherent biofilm formation and 53% Ag:47% Au NPs 34 mM citrate have a 67% frequency of moderately adherent biofilm formation (Table 19).

Table 19 Biofilm adherence of *E. coli* in NPs presence

***E. coli* + NPs**		**Biofilm adherence**		
		Weakly	**Moderately**	**Strongly**
100% Ag 38.8 mM citrate (n=3)	**24 h**	100%	0%	0%
	72 h	0%	33%	67%
80% Ag:20% Au 38.8 mM citrate (n=2)	**24 h**	100%	0%	0%
	72 h	100%	0%	0%
65% Ag:35% Au 38.8 mM citrate (n=3)	**24 h**	0%	0%	100%
	72 h	0%	0%	100%
53% Ag:47% Au 34 mM citrate (n=3)	**24 h**	0%	67%	33%
	72 h	0%	67%	33%

Table 20 shows the results for *S. aureus* in the presence of NPs, where the majority of experiments for every NPs types produced enables biofilm formation with strong adherence.

Table 20 Biofilm adherence of *S. aureus* in NPs presence

***S. aureus* + NPs**		**Biofilm adherence**		
		Weakly	**Moderately**	**Strongly**
100% Ag 38.8 mM citrate (n=4)	**24 h**	0%	25%	75%
	72 h	0%	0%	100%
80% Ag:20% Au 38.8 mM citrate (n=4)	**24 h**	0%	0%	100%
	72 h	0%	0%	100%
65% Ag:35% Au 38.8 mM citrate (n=4)	**24 h**	0%	0%	100%
	72 h	0%	0%	100%
61% Ag:39% Au 34 mM citrate (n=2)	**24 h**	0%	0%	100%
	72 h	0%	50%	50%
53% Ag:47% Au 34 mM citrate (n=2)	**24 h**	0%	0%	100%
	72 h	0%	50%	50%

4.3.3 Inhibition of biofilm growth using antibiotics and NPs together

Biofilm formation of *E. coli* was evaluated using antibiotics and NPs together.

In Table 21 is possible to see that for E. coli with 100% Ag NPs 38.8 mM citrate a weakly adherent biofilm is formed with a frequency of 100% for all the conditions performed, with an exception for 72 h of incubation without antibiotic where 67% of the experiments present a strongly adherent biofilm formation. In Table 21 the 100% frequency of biofilm formation with weakly adherence after 24 h of incubation for all the Km concentrations may correspond to the NPs effect already seen in Table 19.

Table 21 Biofilm adherence of *E. coli* in 100% Ag NPs 38.8 mM citrate presence with Km

***E. coli* + Km + NPs**			**Biofilm adherence**		
			Weakly	**Moderately**	**Strongly**
100% Ag 38.8 mM citrate	**50% MIC (n=2)**	**24 h**	100%	0%	0%
		72 h	100%	0%	0%
	25% MIC (n=2)	**24 h**	100%	0%	0%
		72 h	100%	0%	0%
	0% MIC (n=3)	**24 h**	100%	0%	0%
		72 h	0%	33%	67%

Table 22 presents results for *E. coli* with 80% Ag:20% Au NPs 38.8mM citrate and Km, where in 100% of the experiments a weakly adherent biofilm was formed.

Table 22 Biofilm adherence of *E. coli* in 80% Ag:20% Au NPs 38.8 mM citrate presence with Km

***E. coli* + Km + NPs**			**Biofilm adherence**		
			Weakly	**Moderately**	**Strongly**
80% Ag:20% Au 38.8 mM citrate	**50% MIC (n=2)**	**24 h**	100%	0%	0%
		72 h	100%	0%	0%
	25% MIC (n=2)	**24 h**	100%	0%	0%
		72 h	100%	0%	0%
	0% MIC (n=2)	**24 h**	100%	0%	0%
		72 h	100%	0%	0%

For antibiotic with 65% Ag:35% Au NPs 38.8 mM citrate, antibacterial activity was observed with antibiotic concentrations of 50% MIC and with 25% MIC (Table 23). In Table 23 is possible to observe 50%, 75% and 67% frequency of weakly adherent biofilm formation correspondent to 50% MIC after 24 h and 72 h of incubation and 25% MIC after 72 h of incubation respectively. With 25% MIC after 24 h of incubation moderately adherent biofilm was formed with a 100% frequency.

Table 23 Biofilm adherence of *E. coli* in 65% Ag:35% Au NPs 38.8 mM citrate presence with Km

***E. coli* + Km + NPs**			**Biofilm adherence**		
			Weakly	**Moderately**	**Strongly**
65% Ag:35% Au 38.8 mM citrate	**50% MIC (n=4)**	**24 h**	50%	25%	25%
		72 h	75%	0%	25%
	25% MIC (n=3)	**24 h**	0%	100%	0%
		72 h	67%	0%	33%
	0% MIC (n=3)	**24 h**	0%	0%	100%
		72 h	0%	0%	100%

In Table 24 for 53% Ag:47% Au NPs 34 mM citrate with 50% MIC after 72 h of incubation 67% frequency of weakly adherent biofilm formation was observed, and with 25% MIC after both time points, 100% frequency of weakly adherent biofilm formation was observed. For 0% MIC after both time points the inhibition of biofilm formation seems to be result of NPs antibacterial effect because the same values were obtained in Table 19.

Table 24 Biofilm adherence of *E. coli* in 53% Ag:47% Au NPs 34 mM citrate presence with Km

***E. coli* + Km + NPs**			**Biofilm adherence**		
			Weakly	**Moderately**	**Strongly**
53% Ag:47% Au 34 mM citrate	**50% MIC (n=3)**	**24 h**	0%	100%	0%
		72 h	67%	0%	33%
	25% MIC (n=2)	**24 h**	100%	0%	0%
		72 h	100%	0%	0%
	0% MIC (n=3)	**24 h**	0%	67%	33%
		72 h	0%	67%	33%

Biofilm formation of *S. aureus* was also evaluated using antibiotics and NPs together.

In Table 25 for 100% Ag NPs 38.8 mM citrate with Amp concentration of 50% MIC after 24 h of incubation the presented value of 100% frequency for weakly adherent biofilm formation may be due to the antibiotic effect (**Table 18**). NPs with 50% MIC after 72 h of incubation had 50% of weakly adherent biofilm formation (Table 25). NPs with 25% MIC after 24 h and 72 h of incubation

resulted in 100% and 50% frequencies of weakly adherent biofilm formation respectively (Table 25). In Table 25 for these NPs with 0% MIC after 24 h of incubation a moderately adherent biofilm was formed with 50% frequency.

Table 25 Biofilm adherence of *S. aureus* in 100% Ag NPs 38.8 mM citrate presence with Amp

***S. aureus* + Amp + NPs**			**Biofilm adherence**		
			Weakly	**Moderately**	**Strongly**
100% Ag 38.8 mM citrate (n=2)	**50% MIC**	**24 h**	100%	0%	0%
		72 h	50%	50%	0%
	25% MIC	**24 h**	100%	0%	0%
		72 h	50%	0%	50%
	0% MIC	**24 h**	0%	50%	50%
		72 h	0%	0%	100%

Table 26 shows the results for 80% Ag:20% Au NPs 38.8 mM citrate with antibiotic. For the concentration of 25% MIC after 72 h of incubation a 100% frequency of strongly adherent biofilm formation obtained where no NPs were added (Table 18) was inhibited and replaced for 50% frequencies of weakly and moderately adherent biofilm formation.

Table 26 Biofilm adherence of *S. aureus* in 80% Ag:20% Au NPs 38.8 mM citrate presence with Amp

***S. aureus* + Amp + NPs**			**Biofilm adherence**		
			Weakly	**Moderately**	**Strongly**
80% Ag:20% Au 38.8 mM citrate (n=2)	**50% MIC**	**24 h**	50%	0%	50%
		72 h	0%	0%	100%
	25% MIC	**24 h**	0%	0%	100%
		72 h	50%	50%	0%
	0% MIC	**24 h**	0%	0%	100%
		72 h	0%	0%	100%

In Table 27 the result for 50% MIC after 24 h of incubation with 65% Ag:35% Au NPs 38.8 mM citrate was expected due to Amp antimicrobial effect (Table 18). For these NPs with 25% MIC frequencies of 50% and 100% of moderately adherent biofilm after 24 h and 72 h respectively were observed instead of 100% frequency of strongly adherent biofilm (Table 27).

Table 27 Biofilm adherence of *S. aureus* in 65% Ag:35% Au NPs 38.8 mM citrate presence with Amp

***S. aureus* + Amp + NPs**			**Biofilm adherence**		
			Weakly	**Moderately**	**Strongly**
65% Ag:35% Au 38.8 mM citrate (n=2)	**50% MIC**	**24 h**	100%	0%	0%
		72 h	0%	0%	100%
	25% MIC	**24 h**	0%	50%	50%
		72 h	0%	100%	0%
	0% MIC	**24 h**	0%	0%	100%
		72 h	0%	0%	100%

With 61% Ag:39% Au NPs 34 mM citrate and 25% MIC after 24 h of incubation 50% frequency of weakly adherent biofilm formation was observed and after 72 h 100% frequency of weakly adherent biofilm formation was observed. The 50% frequency of moderately adherent biofilm formation with 50% MIC and 0% MIC after 72 h of incubation may be due to these NPs effect (Table 20).

Table 28 Biofilm adherence of *S. aureus* in 61% Ag:39% Au NPs 34 mM citrate presence with Amp

***S. aureus* + Amp + NPs**			**Biofilm adherence**		
			Weakly	**Moderately**	**Strongly**
61% Ag:39% Au 34 mM citrate (n=2)	**50% MIC**	**24 h**	50%	0%	50%
		72 h	0%	50%	50%
	25% MIC	**24 h**	50%	0%	50%
		72 h	100%	0%	0%
	0% MIC	**24 h**	0%	0%	100%
		72 h	0%	50%	50%

4.4 Effect of PHB/PHV films on *E. coli* and *S. aureus*

PHB/PHV films were prepared to contain NPs and afterwards assays were performed for *E. coli* and *S. aureus* to evaluate the nanomaterial antimicrobial properties. *E. coli* presented a halo around the polymer, but for *S. aureus* no halo was observed (Table 29). Two equal films (A and B) were made for the control and for each type of NPs. The concentration of the NPs used in the polymer was 33.75-fold the concentration indicated in Table 2.

Antimicrobial activity of PHA films with NPs was observed for films containing 100% Ag NPs 38.8 mM citrate by a halo observation with a size of 0.05-0.1 cm (Table 29). Film A with 80% Ag:20% Au NPs 38.8 mM citrate caused a halo with approximately 0.01 cm and with 61% Ag:39% Au NPs 34 mM citrate caused halos with about 0.05 cm.

Table 29 Frequency of antimicrobial effect of PHB/PHV films in *E. coli* through a halo observation

PHBHV Films with Tween 0.5%		**Without NP's**	**With NPs**			
			100% Ag 38.8 mM citrate	**80% Ag:20% Au 38.8 mM citrate**	**65% Ag:35% Au 38.8 mM citrate**	**61% Ag:39% Au 34 mM citrate**
		Halo presence	Halo presence	Halo presence	Halo presence	Halo presence
E. coli incubated at 25ºC	Filme A (n=5)	0%	40%	20%	0%	60%
	Filme B (n=4)	0%	50%	0%	0%	0%
E. coli incubated at 37ºC	Filme A (n=5)	0%	20%	0%	0%	40%
	Filme B (n=4)	0%	25%	0%	0%	0%

4.5 Cytotoxicity of NPs

The toxicity of NPs on human cells was evaluated by the MTT assay. Four types of NPs with different concentration ranges were incubated at 37ºC with the human cells. The concentration range tested was from 541 mg/mL Ag to 0 mg/mL Ag. For all the NPs tested the Ag concentrations indicated correspond to the total Ag amount contained in the NPs suspension. Before NPs adding and cell incubation the cell number per mL was $9.43x10^{05} \pm 1.01x10^{05}$.

After 24 h of incubation of NPs with cells it is possible to observe that 100% Ag NPs 38.8 mM citrate with 541 mg/mL Ag had the highest toxic effect represented by the lowest cell survival (Fig. 34). It is possible to observe for 80% Ag:20% Au NPs 38.8 mM citrate with 541 mg/mL Ag a higher value for normalized cell survival than for the control 0 mg/mL Ag (Fig. 34).

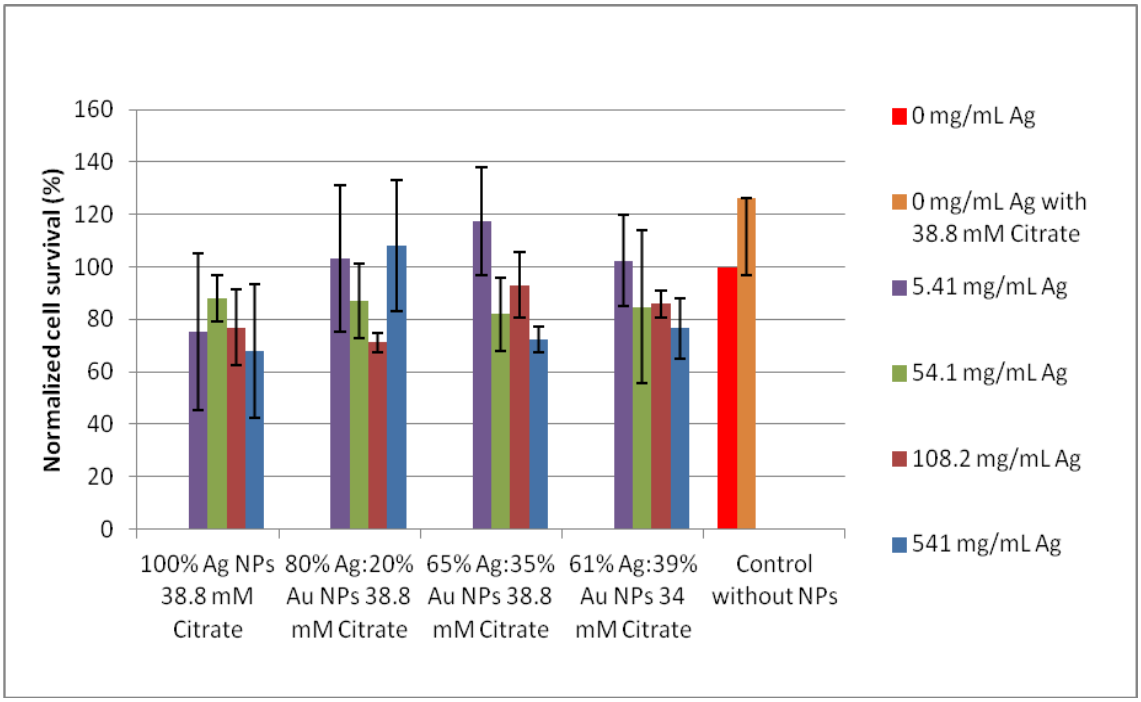

Fig. 34 Cell survival after 24 h of incubation with NPs

After 48 h of incubation of NPs with cells the highest toxic effect is caused by 100% Ag NPs 38.8 mM citrate, with more than 50% difference in the amounts of cell survival between these NPs and controls (Fig. 35). All four kinds of NPs present toxic effect with Ag concentrations of 541 mg/mL and 108.2 mg/mL. The lower toxic effect was observed for 61% Ag:47% Au NPs 34 mM citrate (Fig. 35).

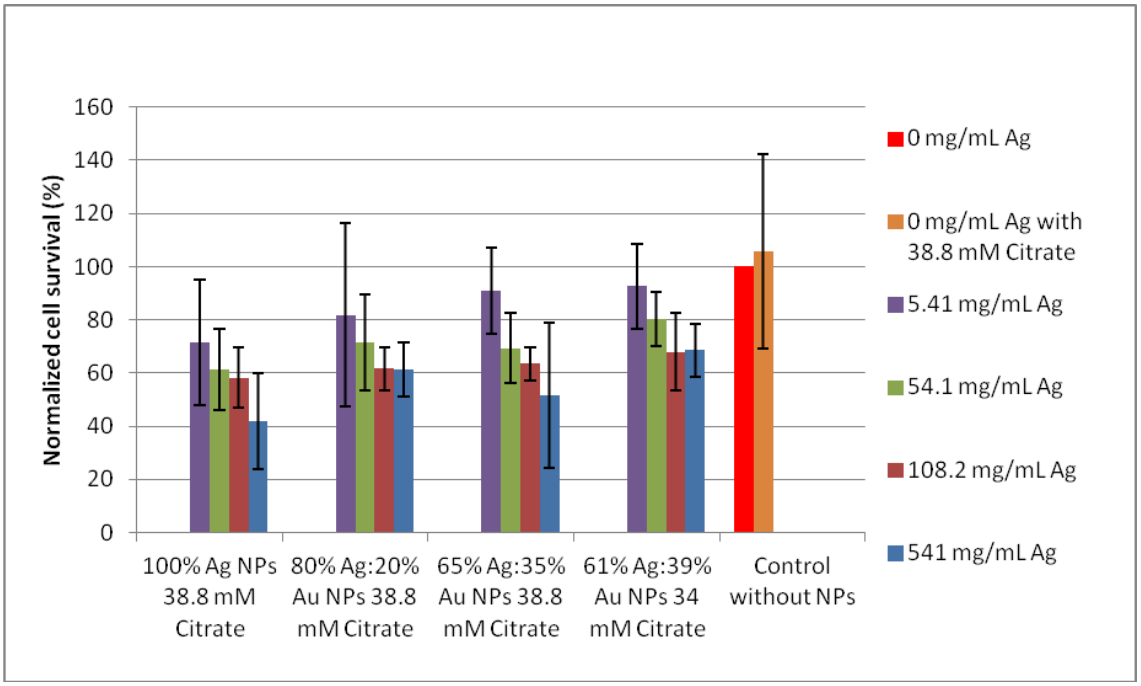

Fig. 35 Cell survival after 48 h of incubation with NPs

In Fig. 36 the MTT assay results after 72 h of incubation are presented. Once again, 100% Ag NPs 38.8 mM citrate with 541 mg/mL of Ag have the higher toxic effect represented by the higher cell death. From 48 h of incubation (Fig. 35) to 72 h of incubation (Fig. 36) only four conditions suffer cell survival decrease - 100% Ag NPs 38.8 mM citrate with 541 mg/mL of Ag; 80% Ag:20% Au NPs 38.8 mM citrate with 541 mg/mL of Ag; 65% Ag:35% Au NPs 38.8 mM citrate with 54.1 mg/mL of Ag and 61% Ag:39% Au NPs 34 mM citrate with 5.41 mg/mL of Ag.

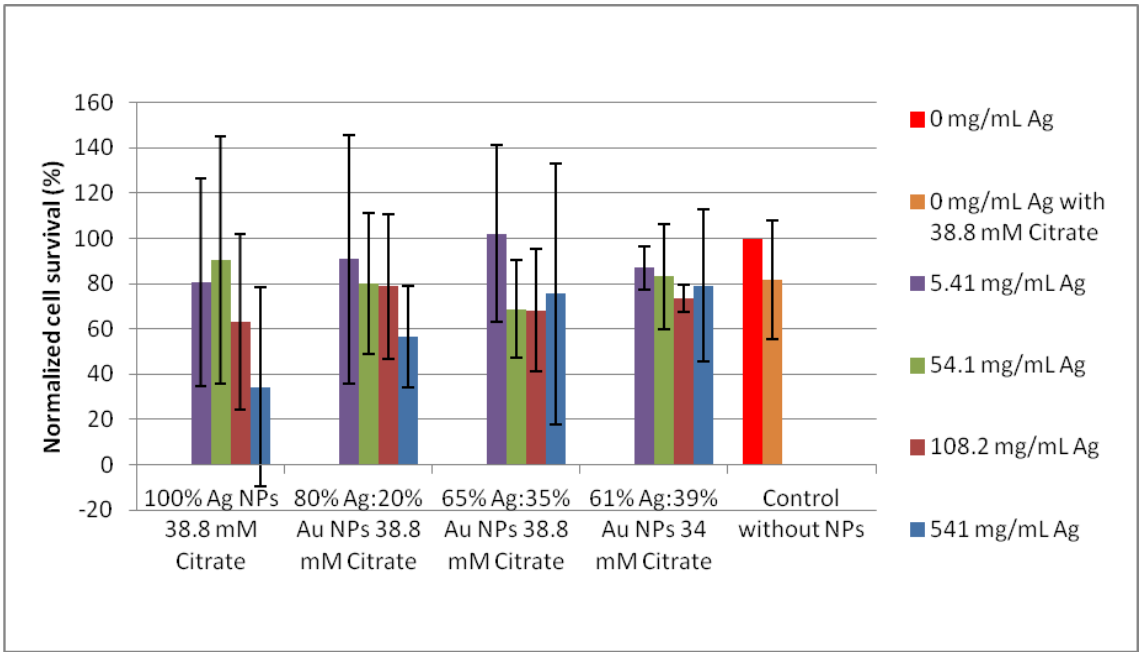

Fig. 36 Cell survival after 72 h of incubation with NPs

Fig. 37 to Fig. 40 show MTT assay results by NPs type in order to evaluate their toxicity over time.

For 100% Ag NPs 38.8 mM citrate the expected decrease of normalized cells survival, because of cell death overtime due to the toxic effect of NPs, is illustrated with one noteworthy exception for Ag concentration of 54.1 mg/mL (Fig. 37).

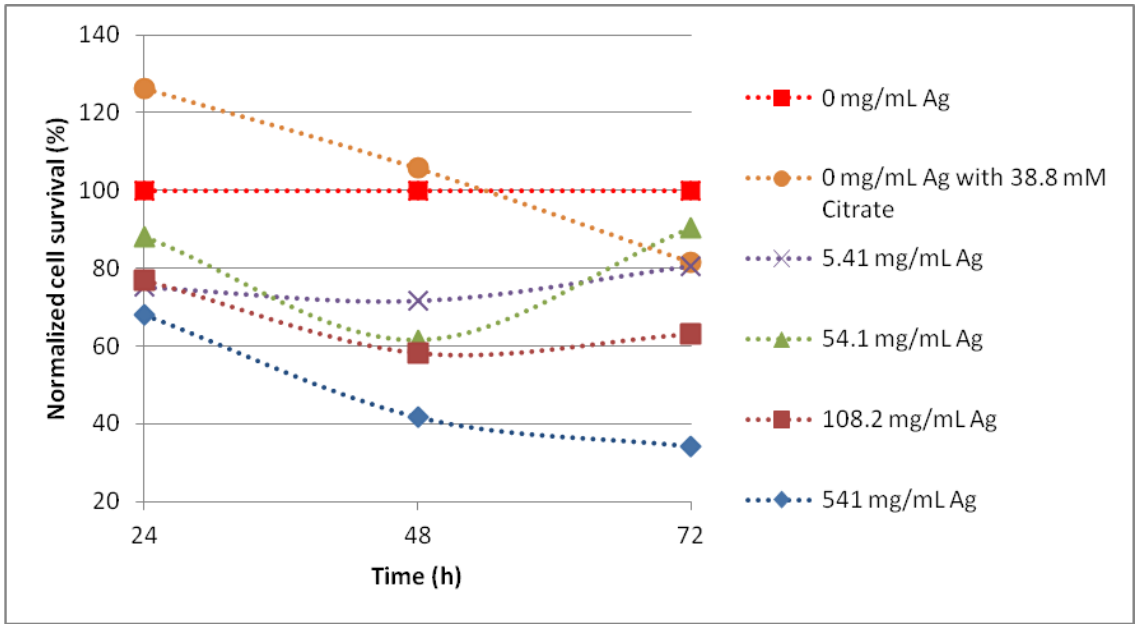

Fig. 37 Cell survival over time until 72 h of incubation with 100% Ag NPs 38.8 mM citrate

In Fig. 38 is possible to see a decrease of normalized cell survival for all Ag concentrations after 48 h, however, after 72 h this decrease is observed only for the maximum Ag concentration.

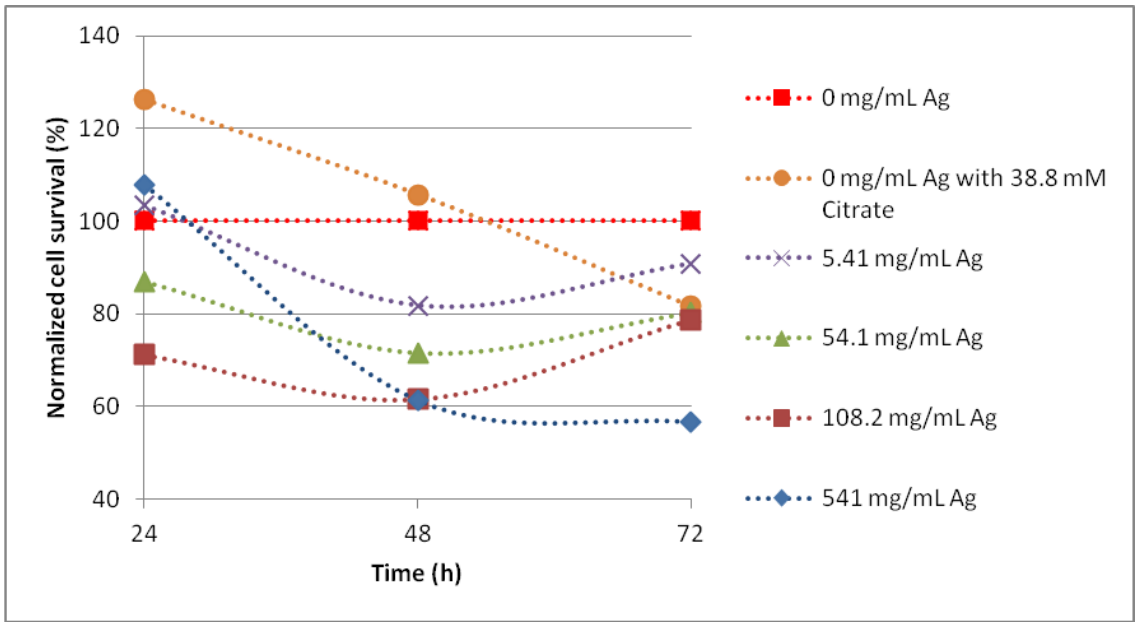

Fig. 38 Cell survival over time until 72 h of incubation with 80% Ag:20% Au NPs 38.8 mM citrate

The results for 65% Ag:35% Au NPs 38.8 mM citrate show that the minimum values for cell survival are reached after 48 h of incubation with an exception for 54.1 mg/mL Ag (Fig. 39).

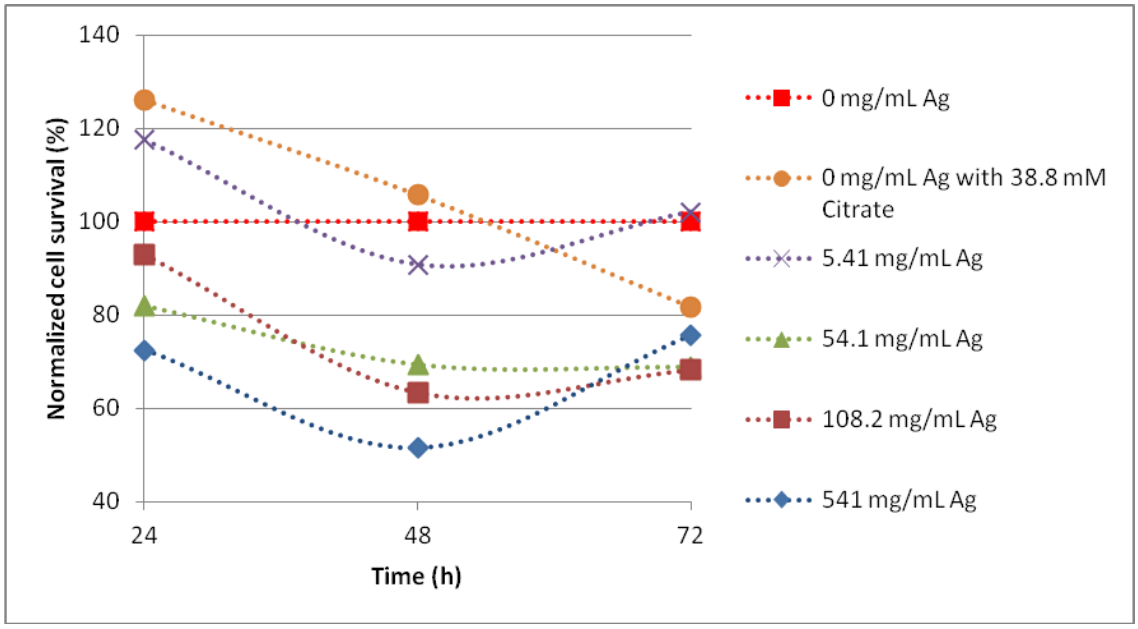

Fig. 39 Cell survival over time until 72 h of incubation with 65% Ag:35% Au NPs 38.8 mM citrate

In Fig. 40 shows the results for 61% Ag:39% Au NPs 34 mM citrate, where is possible to observe a continuous decrease in normalized cell survival values over time only for 5.41 mg/mL Ag.

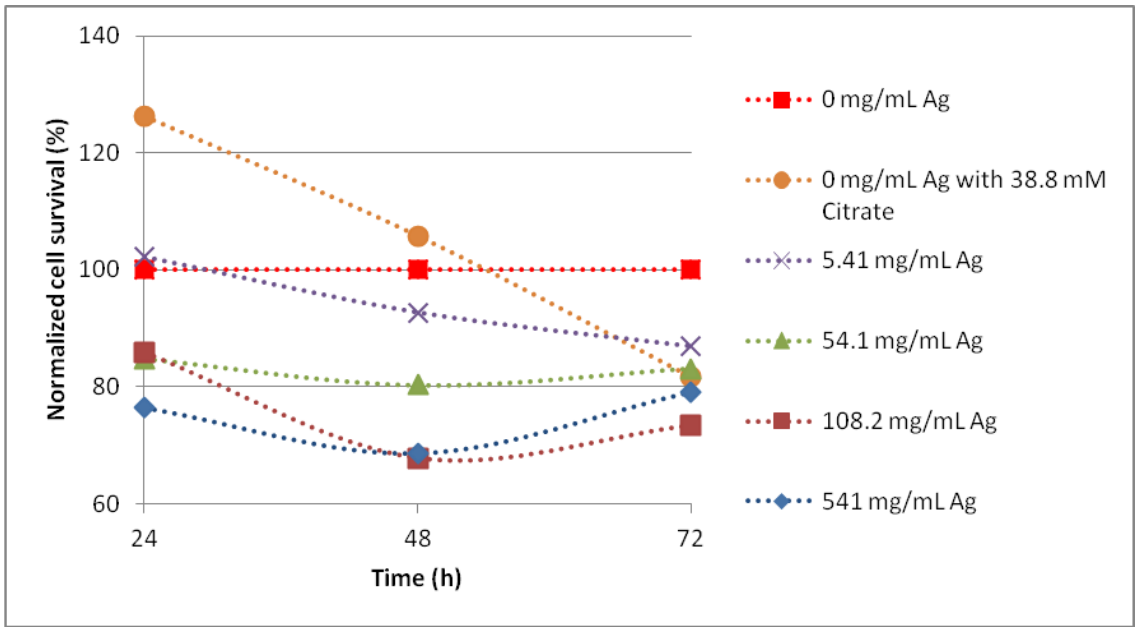

Fig. 40 Cell survival over time until 72 h of incubation with 61% Ag:39% Au NPs 34 mM citrate

4.6 Ecotoxicity of NPs

D. salina growth curve was made in seawater. Fig. 41 shows that these algae grow linearly from 24 h to 92 h and at about 114 h they start to die.

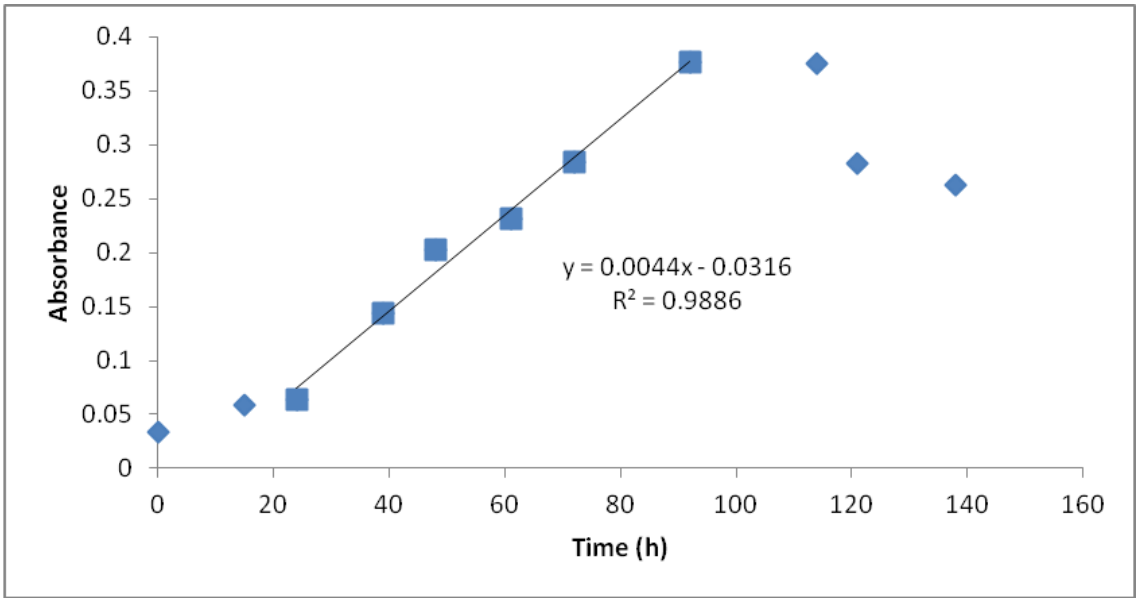

Fig. 41 *D. salina* growth curve in seawater by UV-Vis. evaluation at 680 nm (unpublished results of Miguel Larguinho)

The ecotoxicity of NPs on algae *Dunaliella salina* was evaluated. Four types of NPs with three different concentrations were added to algae in seawater and after different times the number of algae were counted using microscopy. The concentration range tested was from 1 mg/mL Ag to 0 mg/mL Ag. For all the NPs tested the Ag concentrations indicated correspond to the total Ag amount contained in the NPs suspension. Before NPs addition, the algae number was $1.94x10^{06}$/mL ± $6.79x10^{05}$.

After 24 h and 48 h of NPs addition to algae is possible to observe that the lowest cell survival value corresponds to 100% Ag NPs 38.8 mM citrate with a Ag concentration of 1 mg/mL (Fig. 42 and Fig. 43). Fig. 42 shows a gradual decay of *D. salina* survivors for these NPs with the increase of Ag amount, in a dose dependant manner.

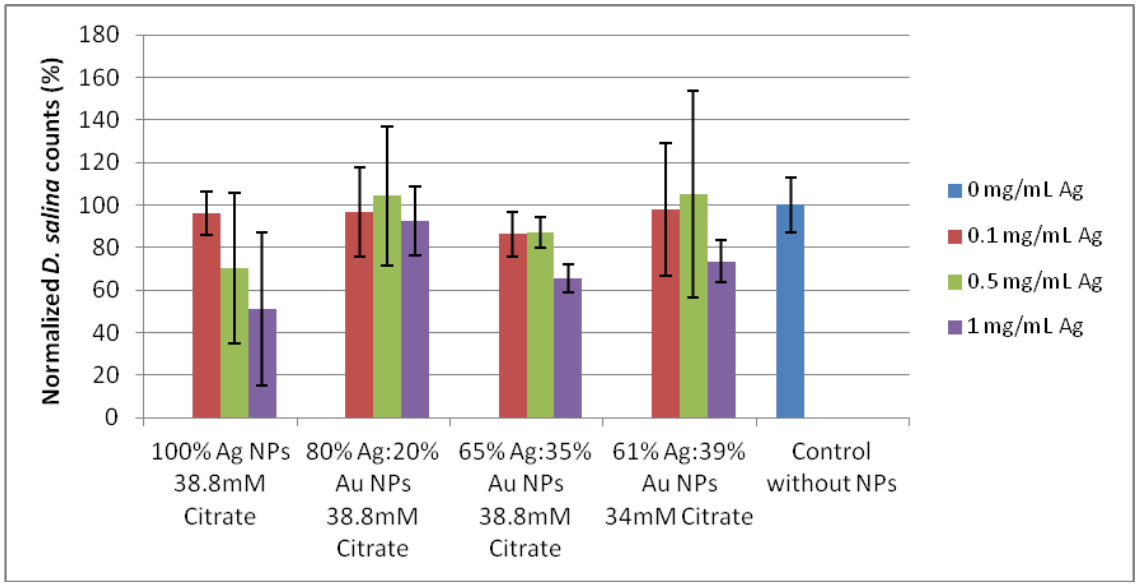

Fig. 42 Normalized *Dunaliella salina* counts after 24 h of NPs addition

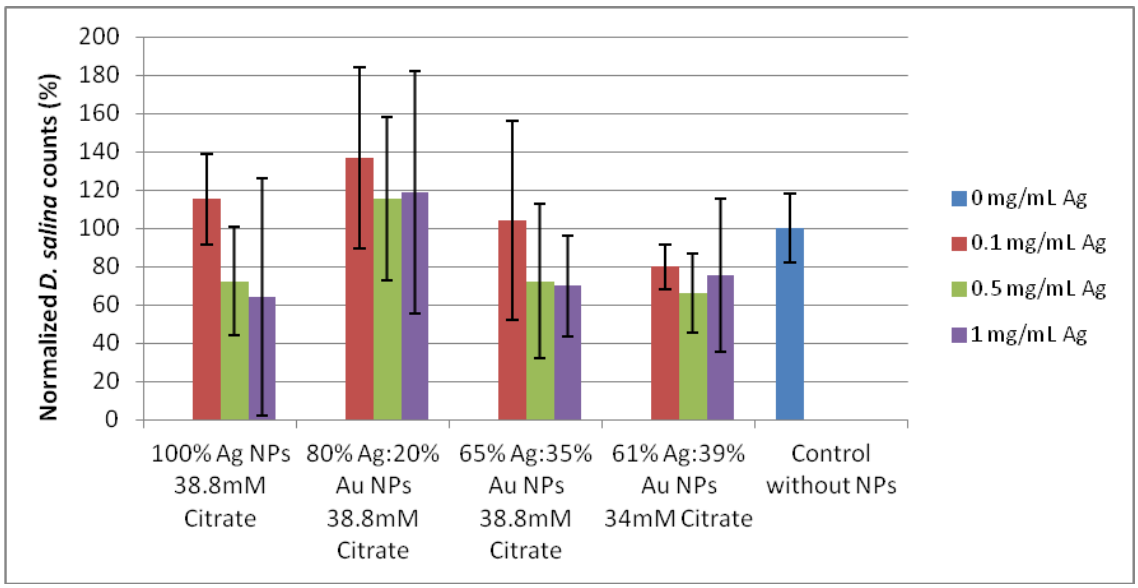

Fig. 43 Normalized *Dunaliella salina* counts after 48 h of NPs addition

All the NPs showed ecotoxic effects on *D. salina* for the Ag dose of 1mg/mL after 24 h and 48 h of exposure (Fig. 42 and Fig. 43).

Chapter 5 – Discussion

In this chapter we will discuss all the results obtained in Chapter 4 according to the thematic theory already described in the State of the Art (Chapter 2).

Noble metal NPs synthesised had different compositions and sizes. These NPs absorbed at the UV-Vis. range as a consequence of the distinct surface plasmon resonances [6,7,8,22]. Differential composition of the produced NPs corresponded to their light plasmon resonance band different wavelengths, where the decrease of Ag amount in NPs shifted the value of maximum absorbance to higher wavelength (Fig. 5) [6,7,8,22]. The obtained scattering results in Fig. 5 are in agreement with literature [6,7,8,11]. This synthesised NPs, with an exception for 100% Ag NPs 38.8mM citrate, corresponded to an alloy-NPs form because their UV-Vis. spectra showed only one plasmon resonance band (Fig. 5) [6,7,8]. NPs different sizes and refractive index of the surrounding media do not perform a significant effect in plasmon resonance band [7,8]. The produced NPs had different distribution sizes that were not correspondent to a normal distribution, hence, besides NPs average size measurement, median size had to be calculated too (Table 12). It has been already studied that beyond NPs chemical composition and shape, size also influences their biological activity [4,17]. In this work, NPs antimicrobial activity will be assessed based on the NPs different compositions, because the NPs sizes were all in the same range, between 30-60 nm. A bacteria has a size in the order of magnitude of 1 µm, the produced NPs had sizes about 22 times lower.

After an evaluation of biofilm formation on a glass surface we conclude that *S. aureus* biofilm was more quickly formed than *E. coli* biofilm. It took about 8 days to *S. aureus* biofilm formation and 12 days to reach the high cell density, while E. coli needed approximately 24 days to go on an adhesive form (Table 13). After a month of continuously incubation the cell density in an adhesive form suffered a great decrease, corresponding to biofilm disassembly (Table 13). The processes that involve biofilm disassembly are not clear yet. However, for Gram-negative bacteria as *E. coli* some factors as starvation or loss of

exopolysaccharides expression might be involved [5]. For Gram-positive bacteria as *S. aureus* the processes of cell detachment might include multiple steps such as extracellular matrix degradation and physiological changes to prepare the organisms to a planktonic life [13]. *S. aureus* disassembly can be triggered by environmental conditions like surface deterioration, nutrients depletion (such as glucose depletion in growth media), accumulation of wastes or antimicrobial compounds [13]. In Fig. 30 to Fig. 33 we observed some possible biofilms structures as clusters, gaps and channels, however, it was difficult to distinguish them.

The biofilm formation was also evaluated in a PVC surface with good nutrient conditions, as rich media and glucose supplementation. After 24 h incubation *E. coli* and *S. aureus* formed a strongly adherent biofilm for 100% of the experiments performed. However, after 72 h of incubation these strains formed a strongly adherent biofilm for the majority of experiments, but not for all of them. As so, we conclude that the growth time may influence biofilm force of adhesion (Table 15 and Table 16).

We were able to prepare two biofilms formation systems. In glass *E. coli* needed about 24 days to form a biofilm, however only 6 days later the biofilm dissembled. *S. aureus* formed a biofilm with higher cell density in about 12 days that dissembled in day 35 (Table 13). In PVC surface we were able to form strong adherent biofilms of both strains in 24 h. Even though there are differences in the inoculum and % glucose between the two systems developed for biofilm formation, we could hypothesise that the surface of adhesion plays an important role in biofilm formation. We were able to achieve biofilm formation in two different surfaces with strains that are not described as biofilm formers.

The NPs anti-adhesive activity was tested for *E. coli* and *S. aureus* (Table 19 and Table 20). The highest antimicrobial effect of NPs for *E. coli* was observed with 100% Ag NPs 38.8 mM citrate after 24 h of incubation and with 80% Ag:20% Au NPs 38.8 mM citrate after both time points through the growth inhibition of strong adherent biofilm that was replaced with 100% frequency of weakly adherent biofilm formation (Table 19). This biofilm growth inhibition may

be due to the higher amount of Ag present in these NPs, an agent that was already been described as antimicrobial [6,8,11,14,17,18]. We cannot assess which was mechanism that caused biofilm growth inhibition; however we can propose a silver ion interference or membrane disturbance by NPs. The 53% Ag:47% Au NPs 34 mM citrate had a weak antimicrobial action as seen by the 67% frequency of moderately adherent biofilm formation instead of strongly adherent biofilm formation in the absence of NPs, that may be due to a lower amount of silver present in the suspension. No antibacterial activity could be observed for the 65% Ag:35% Au NPs 38.8 mM citrate. The produced NPs did not cause *S. aureus* biofilm inhibition by themselves. 61% Ag:39% Au NPs 34 mM citrate and 53% Ag:47% Au NPs 34 mM citrate had a minor antimicrobial effect with a 50% frequency of biofilm formation with moderate adherence (Table 20).

Antibiotics for *E. coli* and *S. aureus* were chosen and their antimicrobial activity was analysed (Table 17 and Table 18). Using the concentrations of the MIC, inhibition of strongly adherent biofilm growth was obtained after incubation. As the concentration of antibiotics decreases, the biofilm formation assumes a stronger adhesion. With antibiotics the influence of the growth time could also be observed, because after 24 h of incubation the antibiotics had better performance than after 72 h of incubation.

The possibility of a synergetic effect between the antibiotics used and the produced NPs was evaluated. For *E. coli,* this effect was observed with 100% Ag NPs 38.8 mM citrate, 65% Ag:35% Au NPs 38.8 mM citrate and 53% Ag:47% Au NPs 34 mM citrate. 100% Ag NPs 38.8 mM citrate with 50% MIC and with 25% MIC after 72 h of incubation decreased the 67% biofilm formation frequency with strong adherence to a 100% frequency of weakly adherent biofilm formation. 65% Ag:35% Au NPs 38.8 mM citrate with 50% MIC after 24h and 72 h of incubation and with 25% MIC after 72 h of incubation decreased the 78%, 67% and 56% respectively frequencies of strongly adherent biofilm formation to 50%, 75% and 67% respectively frequencies of weakly adherent biofilm formation. These NPs with 25% MIC after 24 h of incubation also had a synergetic effect by the reduction of the 78% frequency of strongly adherent biofilm formation to 100% moderately adherence biofilm formation. 53%

Ag:47% Au NPs 34 mM citrate with 50% MIC after 72 h decreased the 67% frequency of moderately adherent biofilm formation to weakly adherent biofilm formation of incubation. These types of NPs with 25% MIC after both time points decreased the 67% frequency of moderately adherent biofilm formation to 100% frequency of weakly adherent biofilm formation. For *S. aureus* the increase of biofilm growth inhibition due to Amp with NPs was observed with all the tested NPs. 100% Ag NPs 38.8 mM citrate with 50% MIC after 72 h of incubation decreased the 50% biofilm formation with strong adherence frequency to 50% frequency of weakly adherent biofilm formation; with 25% MIC after both time points decreased the 75% and 100% frequencies of strongly adherent biofilm formation to 100% and 50% respectively frequencies of weakly adherent biofilm formation. 80% Ag:20% Au NPs 38.8 mM citrate with 25% MIC caused a reduction of the 100% frequency of strongly adherent biofilm formation to 50% frequency of weakly adherent biofilm formation after 24 h of incubation and to a 50% of moderately adherent biofilm formation after 72 h of incubation. 65% Ag:35% Au NPs 38.8 mM citrate with 25% MIC decreased the 100% frequency of strongly adherent biofilm formation to 50% and 100% frequencies of moderately adherent biofilm formation after 24 h and 72 h of incubation respectively. 61% Ag:39% Au NPs 34 mM citrate with 25% MIC after 24 h of incubation decreased the 100% frequency of strongly adherent biofilm formation to 50% frequency of weakly adherent biofilm formation and after 72 h of incubation decreased the 50% frequencies of moderately and strongly adherent biofilm formation to 100% frequency of weakly adherent biofilm formation.

By the previous discussed results we can conclude that all the produced NPs can demonstrate a synergetic activity with antibiotics both for *E. coli* and *S. aureus*. The greatest antimicrobial activity via enhancement of NPs effect with antibiotics was seen with 100% Ag NPs 38.8 mM citrate because a high formation of strongly adherent biofilm was replaced for a 100% frequency of weakly adherent biofilm formation. The superior biofilm growth inhibition obtained with these NPs may be a result of their higher Ag amount. The enhancement of antimicrobial activity of antibiotics with NPs makes it possible

to lower the concentration of antibiotics for the same purpose. Consequently we could use antibiotics that in normal concentrations cause harmful side effects, for instance Km that is ototoxic, and we may use Amp to threat infections cause by resistant *S. aureus* strains.

Since nanomaterials engineering is a field in large expansion, another nanomaterial was prepared and its antimicrobial properties were tested. The NPs antimicrobial action was also evaluated when confined in a polymer as PHB/PHV (Table 29). This composite combines the NPs and polymer properties. The produced PHB/PHV films were soft and flexible as expected [9,10]. Antimicrobial activity was observed only for *E. coli*. Once more, this could indicate that NPs by themselves did not have any antimicrobial action on *S. aureus* as described above in the case of inhibition of biofilm formation with NPs. However, we can question if the method used was the best, because it depended of an antimicrobial activity by the diffusion of the NPs on the agar surface. We do not know the affinity relationship between the NPs and the polymer. So we cannot exclude the possibility of antimicrobial activity of the NPs on *S. aureus* by other mechanism, different from silver ions diffusion, which cannot be observed with this assay. NPs antimicrobial effect was observed on. The most effective NPs for *E. coli* growth inhibition were 100% Ag NPs 38.8 mM citrate with about 45% frequency of halo formation at 25ºC (Film A and Film B) and about 22.5% frequency of halo formation at 37ºC (Film A and Film B) (Table 29). The Ag amount in the NPs may be the most significant factor for antimicrobial activity. Some antimicrobial activity was also observed with 80% Ag:20% Au NPs 38.8 mM citrate and 61% Ag:39% Au NPs 34 mM citrate only for Film A (Table 29). These results demonstrated that the two produced films did not have a similar behaviour as would be expected, so we can speculate that the NPs distribution along the films was not regular. This may evidence that the antimicrobial effect mechanism is trough the Ag^+ ions dispersion into the medium.

We also studied the NPs stability in the different media used along the experiments (Fig. 17 to Fig. 29). When NPs are unstable they aggregate, becoming larger and their surface plasmon resonance band shift to the right

with lower absorbance values than the previous stable maximum wavelength characteristic of the NPs. The light scattering of the aggregated NPs is not characteristic. [6,7,11]. In Fig. 17 to Fig. 29 it was possible to observe that growth media and seawater promotes NPs instability from time zero and consequent progressive aggregation, while in Fig. 16 it could be seen NPs stability in water over time. The produced NPs were aggregated from time zero in seawater and start their aggregation from the same time in the growth media. Therefore, the measured average size for these NPs (Table 12) was not the real size in the experiments. However, this does not present a handicap to this work, since we were evaluating the NPs antimicrobial activity through their Ag:Au composition.

The NPs produced demonstrated to have antimicrobial activity that prevented biofilm formation. Thus it is relevant to evaluate the toxicity associated with these NPs. To evaluate the cytotoxic effect of the produced NPs, a MTT assay was performed with HepG2 cells (Fig. 34 to Fig. 36). This assay establishes a direct proportional relationship between the viable cells with the reduction of MTT reagent to purple formazan [14]. The NPs toxicity is usually associated to their composition, concentration, shape, surface coating and size [23,24,25]. NPs size is one of the factors that influence the cellular uptake, since their physico-chemical properties change [23,25]. For this assay a control without NPs but with the maximum citrate concentration was performed to evaluate the toxicity associated with these NPs capping agent. After 24 h of incubation this control with 38.8 mM citrate had cell viability 26% higher than the control without citrate (Fig. 34). This higher cell viability may be explained due to the citrate significant role in hepatocytes metabolism [28]. A decrease in cell viability was observed over time for this control with 38.8 mM citrate. After 72 h of incubation the number of cell survivors was 18% inferior to the control without citrate (Fig. 36). After all three time points the 100% Ag NPs 38.8 mM citrate with 541 mg/mL Ag proved to be the most toxic. The higher toxic effect for these NPs was after 72 h of incubation with a decrease of about 66% of cell survival (Fig. 36). In general, for all three time points, the less toxic are the 61% Ag:39% Au NPs 34 mM citrate. Since the Ag amount for every type of NPs is the same in these experiment, these toxicity results may be explained through the Ag:Au ratio in

the NPs. When the % Ag is higher in the NPs ratio, the cytotoxicity is higher too. The correlation between the ratio Ag:Au in the NPs and the toxicity can be easily observed after 48 h of incubation and for 541 mg/mL Ag in the NPs after 72 h of incubation (Fig. 35 and Fig. 36). The relationship between dosage and toxicity was easily seen after 48 h of incubation, where the gradual increase of NPs Ag amount, from 0mg/mL Ag until 541 mg/mL Ag, caused a higher cell death (Fig. 35) [6]. The other relationship studied was between incubation time and toxicity. A decrease in cell viability over time was observed for 100% Ag NPs 38.8 mM citrate with 541 mg/mL Ag (Fig. 37) [6] The observed higher value for cell viability in some conditions after 24 h of incubation, rather than in control without citrate, may be explained through the presence of citrate in the NPs (Fig. 34) [28]. Accordingly we may observe a thin balance between the toxicity caused by the upper Ag in Ag:Au ratio with the increase of cell viability possibly caused by the citrate present in the NPs.

The ecotoxicity associated with these NPs was evaluated by exposing the algae *D. salina* to them. A growth curve of these algae performed in seawater proved that this medium was favourable to their growth. From 24 h until 92 h *D. salina* had a linear growth and after 114 h the cells gradually start to die (Fig. 41). The ecotoxicity caused by the NPs may drive from several factors. The main factor may be the NPs chemical composition and aggregation [12]. The NPs are aggregated in seawater (Fig. 29); this was an expected result since the high concentration of salt is one of the factors that cause NPs aggregation [11]. Still, aggregated NPs do not invalidate the interest of the study. The highest ecotoxic effect could be observed with 100% Ag NPs 38.8 mM citrate with 1 mg/mL Ag after 24 h and 48 h with a decrease of 49% and 36% on algae viability respectively (Fig. 42 and Fig. 43). The 80% Ag:20% Au NPs 38.8 mM citrate had a negligible toxic effect on *D. salina.* A correlation between NPs Ag:Au ratio with ecotoxicity could not be observed. Some authors suggest that the surface plasmon resonance of the NPs may increase the intensity of light in the vicinity of the NPs. It would be interesting to study if this putative light increase can increase algae count [7,8,22]. Still, we can also explain this result by the continuously algae growing until 114 h. Ionic strength is one of the favourable

conditions of algae growth, thus we need to take into account the increase of ionic strength caused by the higher volume of seawater in the conditions where the concentration of the NPs was lower.

Chapter 6 – Conclusions

6.1 Conclusions

In this work, two systems for biofilms formation of *E. coli* and *S. aureus*, strains that are not described as biofilm formers, were successfully obtained, one in a glass surface and the other in a PVC surface. Biofilms formation was characterized and we were able to evaluate that for the tested conditions *S. aureus* formed a stronger biofilm in a glass surface and both strains formed a strong adherent biofilm in a PVC surface. We conclude that some factors influenced the biofilm formation as the incubation time and the glucose supplementation.

Different kinds of noble metal-NPs were successfully synthesised and characterised. We were able to prepare NPs with different sizes and concentrations, but with low stability in growth media. The antimicrobial actions of the silver-NPs and Ag:Au alloy-NPs were evaluated on biofilm formation inhibition, as well as their synergic effect with antibiotics for the same purpose. They were also combined with a PHB/PHV polymer and their antimicrobial action by contact evaluated.

The best antimicrobial action was observed through NPs activity for 100% Ag NPs 38.8 mM citrate and 80% Ag:20% Au NPs 38.8 mM citrate on *E. coli* biofilms formation. None of the NPs had a significant inhibition activity for *S. aureus* biofilm formation. A synergic effect between the NPs and the antibiotics Km and Amp was observed for all the NPs types and both *E. coli* and *S. aureus* respectively. The highest combined antimicrobial activity was observed for 100% Ag NPs 38.8 mM citrate. This synergic effect creates a possibility of utilisation of these antibiotics at a lower concentration. Antimicrobial action through contact with a polymeric material composed with NPs was obtained for 100% Ag NPs 38.8 mM citrate. However the prepared equal films did not have the same effect, thus we question if the experimental method was adequate.

The antibacterial mechanism was not evaluated, yet we could suspect that this antimicrobial action may be due to the slow dissolution of Ag^+ ions, because the best inhibition effects were observed with superior % of silver in Ag:Au ratio. We concluded that the best antimicrobial NPs are the silver ones, however they are cytotoxic and ecotoxic. Alloy-NPs as 80% Ag:20% Au NPs 38.8 mM citrate showed good antimicrobial properties too, and the toxicity associated to them were lower. All the NPs prepared had antimicrobial effect under certain conditions.

Nanomaterials as silver NPs and Ag:Au alloy-NPs were able to inhibit biofilm formation and a composite material of polymer and NPs showed antimicrobial properties as well.

6.2 Limitations

This work should have been repeated with pathogenic strains, because they are the main source of nosocomial diseases. However, this could not be performed in the working laboratory because it did not have safety measures to work with this type of bacteria.

There were several material limitations in this work. First, the needed concentration for NPs was very high, and only 275 mL of NPs were synthesised each time. As a result, many sequential centrifugations of 20 min each had to be performed to achieve the NPs concentration needed, in a crowded laboratory. Lastly, not all synthesis ran well, for the reason that it is very difficult to synthesise these NPs types. In addition, three equal syntheses had to be obtained, to reach the necessary final volume to perform all the planned experiments. NPs are frequently used in the laboratory, thus NPs synthesis had to be scheduled.

6.3 Future work

In the future, pathogenic strains or biofilm forming strains should be studied, because every organism is unique, so the biofilm formation should also be unique. If we want to prevent the nosocomial diseases, this study should be repeated with the strains that are the first cause of this health threat.

Other types of NPs should be evaluated for their antimicrobial properties, as well their toxic effects. NPs have a great potential in the biomedical field, so their study may lead to the creation of novel materials that prevent biofilm formation. The prevention may be the best course of action to solve the problem of nosocomial diseases.

An adequate method to inspect antimicrobial and anti-adhesive properties of PHB/PHV films with NPs should be developed, since this material presents good properties to be used in the biomedical field. Other polymeric materials, as chitosan (see Appendix), should also be studied for the same purpose.

Nanoparticles stabilisation with organic or inorganic components should be tacked into account, because the antimicrobial properties of the NPs may be influenced by their aggregation in different media.

Nanotechnology is a promising area for the development of new materials with antimicrobial properties, which may solve big problems like nosocomial diseases, or specific problems in the food industry.

Bibliography

[1] FAO/WHO. Activities on Microbiological Hazards Associates with Fresh Produce. (visualised in http://www.who.int/en/ in 7/10/2013)

[2] WHO. Prevention of hospital-acquired infections – A practical guide. 2nd edition. Geneva. 2002 (visualised in http://www.who.int/en/ in 7/10/2013)

[3] Rubin RJ, Harrington CA, Poon A, Dietrich K, Greene JA, Moiduddin A (1999) The economic impact of *Staphylococcus aureus* infection in New York City Hospitals. Emerg Infect Dis Vol. 5, No. 1

[4] Juan L, Zhimin Z, Anchun M, Lei L, Jingchao Z (2010) Deposition of silver nanoparticles on titanium surface for antibacterial effect. Int J Nanomed 5:216-267

[5] O'Toole G, Kaplan HB, Kolter R (2000) Biofilm formation as microbial development. Annu Rev Microbiol 54:49-79

[6] Mahl D, Diendorf J, Ristig F, Greulich C, Li Z, Farle M, Köller M, Epple M (2012) Silver, gold, and alloyed silver–gold nanoparticles: characterization and comparative cell-biologic action. J Nanopart Res 14:1153

[7] Doria G, Conde J, Veigas B, Giestas L, Almeida C, Assunção M, Rosa J, Baptista PV (2012) Noble metal nanoparticles for biosensing applications. Sensors 12:1657-1687

[8] Link S, Wang ZL, El-Sayed MA (1999) Alloy formation of gold-silver nanoparticles and the dependence of the Plasmon absorption on their composition. J Phys Chem 103:3529-3533

[9] Chen LJ, Wang M (2002) Production and evaluation of biodegradable composites based on PHB–PHV copolymer. Elsevier Biomaterials 23:2631-2639

[10] Otari SV, Ghosh JS (2009) Production and characterization of the polymer polyhydroxy butyrate-co- polyhydroxy valerate by *Bacillus Megaterium* NCIM 2475. J Biolog Sci 1 2: 23-26

[11] Santos MM, Queiroz M, Baptista PV (2012) Enhancement of antibiotic effect via gold:silver-alloy nanoparticles. J Nanopart Res 14:859

[12] Asghari S, Johari SA, Lee JH, Kim YS, Jeon YB, Choi HJ, Moon MC, Yu IJ (2012) Toxicity of various silver nanoparticles compared to silver ions in *Daphnia magna*. J Nanobiotech 10:14

[13] Boles BR, Horswill AR (2011) Staphylococcal biofilm disassembly. Cell Press Vol. 19, No. 9

[14] Jena P, Mohanty S, Mallick R, Jacob B, Sonawane A (2012) Toxicity and antibacterial assessment of chitosan- coated silver nanoparticles on human pathogens and macrophage cells. Int J Nanomed 7:1805–1818

[15] Flemming HC (2002) Biofouling in water systems – cases, causes and countermeasures. Appl Microbiol Biotechnol 59:629–640

[16] Li YH, Tian X (2012) Quorum sensing and bacterial social interactions in biofilms. Sensors 12:2519-2538

[17] Seil JT, Webster TJ (2012) Antimicrobial applications of nanotechnology: methods and literature. Int J Nanomed 7:2767-2781

[18] Radzig MA, Nadtochenko VA, Koksharova OA, Kiwi J, Lipasova VA, Khmel IA (2013) Antibacterial effects of silver nanoparticles on gram-negative bacteria: Influence on the growth and biofilms formation, mechanisms of action. Colloids Surf B Biointerfaces 102:300-306

[19] https://www.google.pt/search?hl=pt-PT&site=imghp&tbm=isch&source=hp&biw=1366&bih=673&q=gram+%2B+e+gram+-&oq=gram+&gs_l=img.1.3.0l6j0i24l4.1611.4042.0.7545.5.5.0.0.0.0.169.755.0j5.5.0....0...1ac.1.29.img..0.5.751.KJ6U6WI7_MU#facrc=_&imgdii

=_&imgrc=UtTPQoAW33fD9M%3A%3BjFyQOrlIRAzgIM%3Bhttp%253A%252F%252Fwww.americanaquariumproducts.com%252Fimages%252Fgraphics%252Fbacteria.jpg%3Bhttp%253A%252F%252Fwww.americanaquariumproducts.com%252Faquarium_medication.html%3B445%3B312 (visualised in 28/10/2013)

[20] http://www.cdc.gov/ecoli/general/index.html (visualised in 28/10/2013)

[21] http://www.cdc.gov/HAI/organisms/staph.html (visualised in 28/10/2013)

[22] Doria G, Larguinho M, Dias JT, Pereira E, Franco R, Baptista PV (2010) Gold–silver-alloy nanoprobes for one-pot multiplex DNA detection. Nanotechnology 21:255101 (5pp)

[23] Albanese A, Chan WCW (2011) Effect of gold nanoparticle aggregation on cell uptake and toxicity. ACS Nano Vol. 5, No. 7:5478–5489

[24] Bachand GD, Allen A, Bachand M, Achyuthan KE, Seagrave JC, Brozik SM (2012) Cytotoxicity and inflammation in human alveolar epithelial cells following exposure to occupational levels of gold and silver nanoparticles. J Nanopart Res 14:1212

[25] Cho EC, Zhang Q, Xia Y (2011) The effect of sedimentation and diffusion on cellular uptake of gold nanoparticles. Nat Nanotech Vol. 6

[26] Turkevich J (1985) Colloidal gold Part I: Historical and preparative aspects, morphology and structure. Gold Bull 18 (3)

[27] Stepanović S, Vuković D, Dakić I, Savić V, Svabić-Vlahović M (2000) A modified microtiter-plate test for quantification of staphylococcal biofilm formation. Elsevier J Microbio Met 40:175–179

[28] Sun J, Aluvila S, Kotaria R, Mayor JA, Walters DE, Kaplan RS (2010) Mitochondrial and plasma membrane citrate transporters: discovery of selective inhibitors and application to structure/function analysis. Mol Cell Pharmacol 2 3:101-110

[29] Dash M, Chiellini F, Ottenbrite RM, Chiellini E (2011) Chitosan - A versatile semi-synthetic polymer in biomedical applications. Prog Polym Sci 36:981-1014

[30] Jena P, Mohanty S, Mallick R, Jacob B, Sonawane A (2012) Toxicity and antibacterial assessment of chitosancoated silver nanoparticles on human pathogens and macrophage cells. Int J Nanomed 7:1805-1818

Appendix

Chitosan

Chitosan is a polymer with large utility in biomedicine because it has some valuable properties. Chitosan might be used in tissue, bone and cartilage engineering, in wounds treatment and as a transport system for antibiotics and other drugs such as hormones, proteins and vaccines [29,30]. Nowadays other applications of chitosan are being explored due to the success of this material in the biomedical field and because it is a linear polymer which drives from chitin, which occurs abundantly in nature. This biomaterial is polycationic, hemostatic and insoluble at high pH. It exhibits properties such as biocompatibility, biodegradability, ecological safety, antimicrobial action and low immunogenicity [29,30]. Chitosan is FDA approved because besides being not toxic, it does not cause allergic and inflammatory reactions after administration, implantation, application or ingestion [29,30]. Due to all this set of characteristics and to the applicability that chitosan presents this material has a growing interest for the purpose of this work, by being a matrix for NPs.

Chitosan films

Preparation of chitosan films

A solution of 2% chitosan in 1% glacial acetic acid was prepared with continuous stirring at 37ºC for approximately 6 h. Then, about 19.5 mL of the homogenous mixture was placed in a Petri dish that was not completely covered to allow for solvent evaporation overnight. The films that were made contained approximately 0.4 g of chitosan.

Preparation of chitosan films with NPs

Chitosan films with NPs contained NPs concentrated from 6.75 mL by two centrifugations at 14500 rpm for 20 min in a micro centrifuge Certomat IS Sartorius. 10 µL of the concentrated NPs were mixed with the chitosan solution before it was placed in the Petri dish.

Antimicrobial activity of chitosan films

An overnight grown culture was 1:100 diluted in phosphate buffer 100 mM pH 7 (27.6 g/L $NaH_2PO_4.H_2O$ (MERK), 53.62 g/L $Na_2HPO_4.7H_2O$ (Fluka Analytical) in an eppendorf. A round piece of chitosan film with or without NPs with approximately 2 mg was placed in the eppendorf that was then incubated at 37ºC for 2 h, 6 h or 24 h. After each time point 100 µL of suspension was plated in rich media (LB or TSB). The plates were incubated at 37ºC overnight and then the CFUs were counted. All the necessary dilutions for CFU counting were performed in phosphate buffer 100 mM pH 7. Duplicate determinations were performed for each condition of the realised experiment.

Effect of chitosan films on *E. coli* and *S. aureus*

Both *E. coli* and *S. aureus* strains were incubated for 24 h with chitosan films with our without different NPs types. The concentration of the NPs was 33.75-fold the concentration indicated in Table 2.

In Fig. 44 it is possible to observe that chitosan films with NPs inhibited *E. coli* growth for a maximum of 80% for a film containing 65% Ag:35% Au NPs 38.8 mM citrate. The film containing 80% Ag:20% Au NPs 38.8 mM citrate inhibited this strain growth for 60%, the minimum antibacterial activity observed.

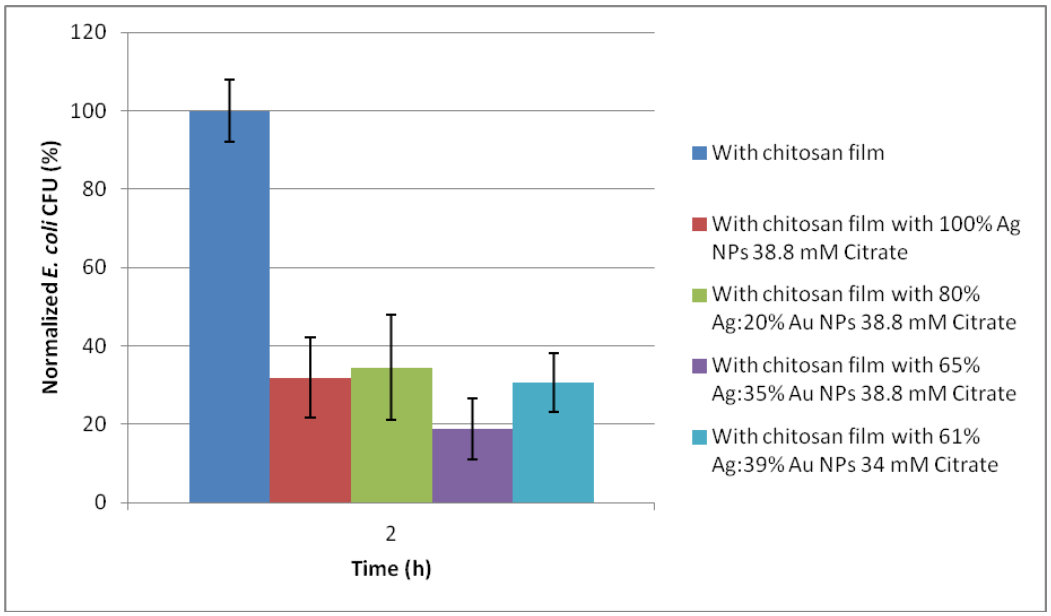

Fig. 44 CFU of *E. coli* after 24 h of incubation with chitosan films

In Fig. 45 it is possible to observe that a chitosan film without NPs has the same effect in *S. aureus* as the control without the chitosan film. 61% Ag:39% Au NPs 34 mM citrate had the maximum antimicrobial action for *S. aureus* with about 50% growth inhibition. A gradual decrease in *S. aureus* viability could be observed with the augment of gold ratio in the NPs (Fig. 45).

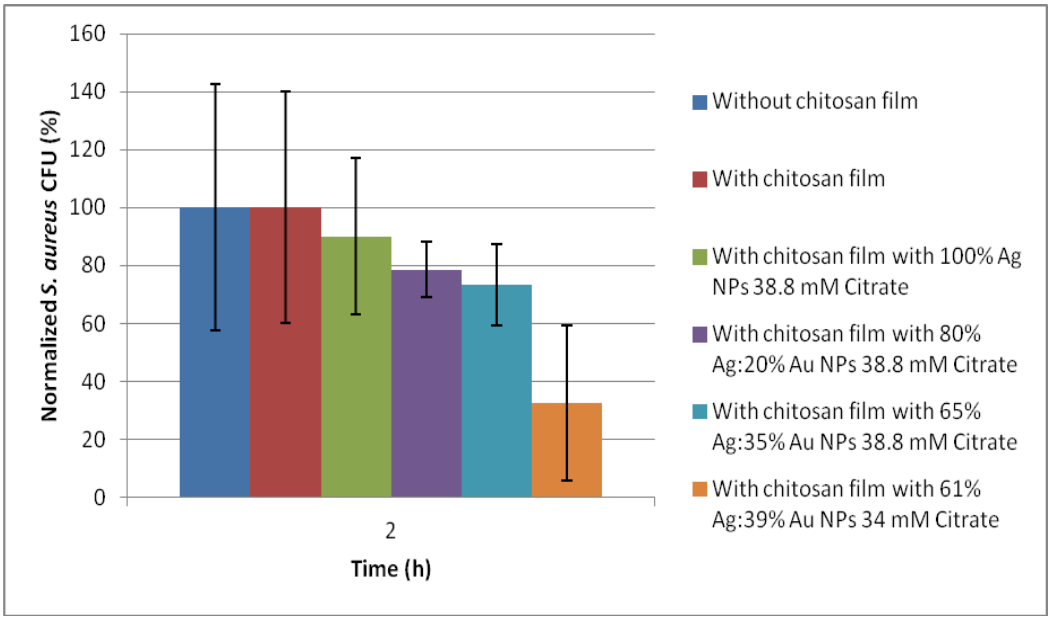

Fig. 45 CFU of *S. aureus* after 24 h of incubation with or without chitosan films

The experiment method used to evaluate the antimicrobial properties of chitosan film containing NPs may not be the appropriate, because it is very difficult to obtain replicable results with the CFU counts. Beyond that, a large quantity of material is spent to obtain duplicates for each condition. Therefore this method should be optimized.